

Stars as thermonuclear reactors: their fuels and ashes¹

A. Ray

Tata Institute of Fundamental Research, Mumbai 400 005, India; akr@tifr.res.in

ABSTRACT

Atomic nuclei are transformed into each other in the cosmos by nuclear reactions inside stars: – the process of nucleosynthesis. The basic concepts of determining nuclear reaction rates inside stars and how they manage to burn their fuel so slowly most of the time are discussed. Thermonuclear reactions involving protons in the hydrostatic burning of hydrogen in stars are discussed first. This is followed by triple alpha reactions in the helium burning stage and the issues of survival of carbon and oxygen in red giant stars connected with nuclear structure of oxygen and neon. Advanced stages of nuclear burning in quiescent reactions involving carbon, neon, oxygen and silicon are discussed. The role of neutron induced reactions in nucleosynthesis beyond iron is discussed briefly, as also the experimental detection of neutrinos from SN1987A which confirmed broadly the ideas concerning gravitational collapse leading to a supernova.

Subject headings: nuclear reactions, nucleosynthesis, abundances; stars: interiors; (stars:) supernovae: general; neutrinos;

PACS: 26.20.+f, 26.30.+k, 26.50.+x 95.30.-k

1. Introduction

Most people do not think of the sun as a star and few would consider stars as nuclear reactors. Yet, not only that is the way it is, even our own world is made out of the “fall-out” from stars that blew up and spewed radioactive debris into the nascent solar system.

Nuclear Astrophysics is the field concerning “the synthesis and Evolution of atomic nuclei, by thermonuclear reactions, from the Big Bang to the present (1). What is the origin

¹Lecture notes on the 5th SERC School on Nuclear Physics, at Panjab University, Chandigarh, Feb 11 - Mar 2, 2002, appearing in “Radioactive Ion Beams and Physics of Nuclei away from the Line of Stability” (eds. Indra M. Govil and Rajiv K. Puri, Elite Publishing House, New Delhi 2003).

of the matter of which we are made?”. Our high entropy universe, presumably resulting from the Big Bang, contains many more photons per particle of matter with mass, e.g. electrons, protons and neutrons. Because of the high entropy and the consequent low density of matter (on terrestrial or stellar scales) at any given temperature as the universe expanded, there was time to manufacture elements only upto helium and the major products of cosmic nucleosynthesis remained hydrogen and helium². Stars formed from this primordial matter and they used these elements as fuel to generate energy like a giant nuclear reactor. In the process, the stars could shine and manufacture higher atomic number elements like carbon, oxygen, calcium and iron of which we and our world is made. The heavy elements are either dredged up from the core of the star to the surface of the star from which they are dispersed by stellar wind or directly ejected into the interstellar medium when a (massive) star explodes. The stardust is the source of heavy elements for new generation of stars and sun-like systems.

The sun is slowly burning a light element, namely, hydrogen into a heavier element, helium. It is not exactly the same now as it just started burning hydrogen in its core and will start to look noticeably different once it exhausts all the hydrogen it *can* burn in its core. In other words, nuclear reactions in the interiors of stars determine the evolution or the life-cycle of the stars, apart from providing them with internal power for heat and light and manufacturing all the heavier elements that the early universe could not.

Since nuclear astrophysics is not usually taught at the master’s level nuclear physics specialisation in our universities, these lecture notes are meant to be an introduction to the subject and a pointer to literature and internet resources. (See for example, (31) for a course of nuclear astrophysics, and the International Conference Proceedings under the title: “Nuclei in the Cosmos” for periodic research conferences in the field. Valuable nuclear astrophysics datasets in machine readable forms useful for researchers can be found at sites:(44), (45). Much of the material discussed here can be found in textbooks in the subject, see e.g. (49), (21), (47), (6), (1) etc.). The emphasis here is on the nuclear reactions in the stars and how these are calculated, rather than how stars evolve. The latter usually form a core area of stellar astrophysics. There is a correspondence between the evolutionary state of a star, its external appearance and internal core conditions and the nuclear fuel it burns, – a sort of a mapping between the astronomers Hertzsprung-Russel diagram and the nuclear physicist’s chart of the nuclides, until nuclear burning takes place on too rapid a timescale –

²Note however suggestions ((17), (16)) that early generation of stars called Pop III objects can also contribute to the abundance of ${}^4\text{He}$ seen in the universe today and therefore the entire present helium may not be a product of big bang nucleosynthesis only, – further aggravating the problems of theoretical predictions of standard big bang nucleosynthesis compared to observed abundances ((55)).

see Reeves (47). This article is organised essentially in the same sequence that a massive star burns successively higher atomic number elements in its core, until it collapses and explodes in a supernova. The introductory part discusses how the rates of thermonuclear reactions in stars are calculated, what the different classes of reactions are and how the stars (usually) manage to burn their fuels so slowly.

2. Stars and their thermonuclear reactions

While referring to Sir Ernest Rutherford “breaking down the atoms of oxygen and nitrogen, driving out an isotope of helium from them”, Arthur Eddington remarked: “what is possible in the Cavendish Laboratory may not be too difficult in the sun” (24). Indeed this is the case, but for the fact that a star does this by fusion reactions, rather than spallation reactions, – in the process giving out heat and light and manufacturing fresh elements. Of all the light elements, hydrogen is the most important one in this regard, because: a) it has a large universal abundance, b) considerable energy evolution is possible with it because of the large binding energies of nuclei that can be generated from its burning and c) its small charge and mass allows it to penetrate easily through the potential barriers of other nuclei. A long term goal of terrestrial plasma physicists has been to achieve a sustained and controlled thermonuclear fusion at economical rates in the laboratory. A star burns its fuel in the core quite naturally via similar thermonuclear reactions, where the confinement of the fuel is achieved in the star’s own gravitational field. These reactions remain “controlled”, or self-regulated, as long as the stellar material remains non-degenerate. (There are however examples to the contrary when a whole white dwarf (resulting from an evolved intermediate mass star) undergoes merger with another and explodes, as nuclear fuel (carbon) is ignited under degenerate conditions, such as in a type Ia supernova).

The recognition of the quantum mechanical tunneling effect prompted Atkinson and Houtermans (3) to work out the qualitative treatment of energy production in stars. They suggested (“how to cook a nucleus in a pot”) that the nucleus serves as both a cooking pot and a trap. Binding energy difference of four protons and two electrons (the nuclear fuel) and their ash, the helium nucleus, some 26.7 MeV is converted to heat and light that we receive from the sun³. The photons in the interior are scattered many a times, for tens of millions of

³Lord Kelvin surmised in the nineteenth century that the solar luminosity is supplied by the gravitational contraction of the sun. Given the solar luminosity, this immediately defined a solar lifetime (the so-called Kelvin-Helmholtz time): $\tau_{KH} = GM_{\odot}^2/R_{\odot}L_{\odot} \sim \text{few} \times 10^7 \text{yr}$. This turned out to be much shorter than the estimated age of the earth at that time known from fossil records, and led to a famous debate between Lord Kelvin and the fossil geologist Cuvier. In fact, as noted above modern estimates of earth’s age are much

years, before they reach the surface of the sun. Some of the reactions also produce neutrinos, which because of their small cross-section for interaction, are not stopped or scattered by overlying matter, – but just stream out straight from the core. Neutrinos therefore are best probes of the core of the star ((23), (33)), while the photons bear information from their surface of last scattering – the photosphere of the star.

2.1. Why do the stars burn slowly: a look at Gamow peaks

The sun has been burning for at least 4.6 billion years⁴. How does it manage to burn so slowly⁵? Under the ambient conditions in the core, the relevant thermonuclear reaction cross

longer and therefore the need to maintain sunshine for such a long time requires that the amount of energy radiated by the sun during its lifetime is much larger than its gravitational energy or its internal (thermal) energy: $L_{\odot} \times t_{life} \gg GM_{\odot}^2/R_{\odot}$. This puzzle was resolved only later with the realisation that the star can tap its much larger nuclear energy reservoir in its core through thermonuclear reactions. The luminosity of the sun however is determined by an interplay of atomic and gravitational physics that controls the opacity, chemical composition, the balance of pressure forces against gravity, etc. Nuclear physics determines how fast nuclear reactions should go under the ambient conditions which regulate through feedback control those reaction rates.

⁴Lord Rutherford (50) determined the age of a sample of pitchblende, to be 700 million years, by measuring the amount of uranium and radium and helium retained in the rock and by calculating the annual output of alpha particles. The oldest rock found is from Southwest Greenland: ≈ 3.8 Gyr old (6). Radioactive dating of meteorites point to their formation and the solidification of the earth about 4.55 ± 0.07 years ago (38). Since the sun and the solar system formed only slightly before, their age at isolation and condensation from the interstellar medium is taken to be 4.6 Gyr (27).

⁵The Nobel prize citation of Hans Bethe (1967) who solved this problem, noted: ” This year’s Nobel Prize in Physics - to professor Hans A. Bethe - concerns an old riddle. How has it been possible for the sun to emit light and heat without exhausting its source not only during the thousands of centuries the human race has existed but also during the enormously long time when living beings needing the sun for their nourishment have developed and flourished on our earth thanks to this source? The solution of this problem seemed even more hopeless when better knowledge of the age of the earth was gained. None of the energy sources known of old could come under consideration. Some quite unknown process must be at work in the interior of the sun. Only when radioactivity, its energy generation exceeding by far any known fuel, was discovered, it began to look as if the riddle might be solved. And, although the first guess that the sun might contain a sufficient amount of radioactive substances soon proved to be wrong, the closer study of radioactivity would by and by open up a new field of physical research in which the solution was to be found. A very important part of his work resulted in eliminating a great number of thinkable nuclear processes under the conditions at the centre of the sun, after which only two possible processes remained..... (Bethe) attempted a thorough analysis of these and other thinkable processes necessary to make it reasonably certain that these processes, and only these, are responsible for the energy generation in the sun and similar stars. ”

sections are very small⁶. For reactions involving charged particles, nuclear physicists often encounter cross-sections near the Coulomb barrier of the order of millibarns. One can obtain a characteristic luminosity L_C based on this cross section and the nuclear energy released per reaction (6) :

$$L_C \sim \epsilon N \Delta E / \tau_C$$

where $\epsilon \approx 10^{-2}$ is the fraction of total number of solar nuclei $N \sim 10^{57}$ that take part in nuclear fusion reactions generating typically $\Delta E \sim 25$ MeV in hydrogen to helium conversion. Here, the τ_C is the characteristic timescale for reactions, which becomes miniscule for the cross-sections at the Coulomb barrier and the ambient density and relative speed of the reactants etc:

$$\tau_C \sim \frac{1}{n\sigma v} = \frac{10^{-8}s}{[n/(10^{26}\text{cm}^{-3})][\sigma/1\text{mbarn}][v/10^9\text{cms}^{-1}]}$$

This would imply a characteristic luminosity of $L_c \approx 10^{20} L_\odot$, even for a small fraction of the solar material taking part in the reactions (i.e. $\epsilon \sim 10^{-2}$). If this were really the appropriate cross-section for the reaction, the sun would have been gone very quickly indeed, Instead the cross-sections are much less than that at the Coulomb barrier penetration energy (say at proton energies of 1 MeV), to allow for a long lifetime of the sun (in addition, weak-interaction process gives a smaller cross-section for some reactions than electromagnetic process, – see Section 3.1).

Stellar nuclear reactions can be either: a) charged particle reactions (both target and projectile are nuclei) or b) neutral particle (neutron) induced reactions. Both sets of reactions can go through either a resonant state of an intermediate nucleus or can be a non-resonant reaction. In the former reaction, the intermediate state could be a narrow unstable state, which decays into other particles or nuclei. In general, a given reaction can involve both types of reaction channels. In charged particle induced reactions, the cross-section for both reaction mechanisms drops rapidly with decreasing energy, due to the effect of the Coulomb barrier (and thus it becomes more difficult to measure stellar reaction cross-sections accurately). In contrast, the neutron induced reaction cross-section is very large and increases with decreasing energy (here, resonances may be superposed on a smooth non-resonant yield which follows the $1/v \sim 1/\sqrt{E}$ dependence). These reaction rates and cross-sections can be then directly measured at stellar energies that are relevant (if such nuclei are long lived or can be generated). The schematic dependence of the cross-sections are shown in Fig. 1.

⁶This makes the experimental verification of the reaction cross-sections a very challenging task, requiring in some cases, extremely high purity targets and projectiles so that relevant small event rates are not swamped by other reaction channels and products (see Rolfs and Rodney, Chapter 5 (49)).

2.2. Gamow peak and the astrophysical S-factor

The sun and other “main-sequence” stars (burning hydrogen in their core quiescently) evolve very slowly by adjusting their central temperature such that the average thermal energy of a nucleus is small compared to the Coulomb repulsion an ion-ion pair encounters. This is how stars can live long for astronomically long times. A central temperature $T \geq 10^7\text{K}$ (or $T_7 \geq 1$, hereafter a subscript x to temperature or density, indicates a temperature in units of 10^x) is required for sufficient kinetic energy of the reactants to overcome the Coulomb barrier and for thermonuclear reactions involving hydrogen to proceed at an effective rate, even though fusion reactions have positive Q values i.e. net energy is liberated out of the reactions. The classical turning point radius for a projectile of charge Z_2 and kinetic energy E_p (in a Coulomb potential $V_C = Z_1Z_2e^2/r$, and effective height of the Coulomb barrier $E_C = Z_1Z_2e^2/R_n = 550\text{ keV}$ for a $p + p$ reaction), is: $r_{cl} = Z_1Z_2e^2/E_p$. Thus, classically a $p + p$ reaction would proceed only when the kinetic energy exceeds 550 keV. Since the number of particles traveling at a given speed is given by the Maxwell Boltzmann (MB) distribution $\phi(E)$, only the tail of the MB distribution above 550 keV is effective when the typical thermal energy is 0.86 keV ($T_9 = 0.01$). The ratio of the tails of the MB distributions: $\phi(550\text{ keV})/\phi(0.86\text{ keV})$ is quite miniscule, and thus classically at typical stellar temperatures this reaction will be virtually absent.

Although classically a particle with projectile energy E_p cannot penetrate beyond the classical turning point, quantum mechanically, one has a finite value of the squared wave function at the nuclear radius $R_n : |\psi(R_n)|^2$. The probability that the incoming particle penetrates the barrier is:

$$P = \frac{|\psi(R_n)|^2}{|\psi(R_c)|^2}$$

where $\psi(r)$ are the wavefunctions at corresponding points. Bethe (10) solved the Schroedinger equation for the Coulomb potential and obtained the transmission probability:-

$$P = \exp\left(-2KR_c\left[\frac{\tan^{-1}(R_c/R_n - 1)^{1/2}}{(R_c/R_n - 1)^{1/2}} - \frac{R_n}{R_c}\right]\right)$$

with $K = [2\mu/\hbar^2(E_c - E)]^{1/2}$. This probability reduces to a much simpler relation at the low energy limit: $E \ll E_c$, which is equivalent to the classical turning point R_c being much larger than the nuclear radius R_n . The probability is:

$$P = \exp(-2\pi\eta) = \exp[-2\pi Z_1Z_2e^2/(\hbar v)] = \exp[-31.3Z_1Z_2(\frac{\mu}{E})^{1/2}]$$

where in the second equality, μ is the reduced mass in Atomic Mass Units and E is the centre of mass energy in keV. The exponential quantity involving the square brackets in the second expression is called the “Gamow factor”. The reaction cross-section between particles of charge Z_1 and Z_2 has this exponential dependence due to the Gamow factor. In addition, because the cross-sections are essentially “areas”: proportional to $\pi(\lambda/2\pi\hbar)^2 \propto 1/E$, it is customary to write the cross-section, with these two energy dependences filtered out:

$$\sigma(E) = \frac{\exp(-2\pi\eta)}{E} S(E)$$

where the factor $S(E)$ is called the astrophysical (or nuclear) S-factor. The S-factor may contain degeneracy factors due to spin, e.g. $[(2J + 1)/(2J_1 + 1)(2J_2 + 1)]$ as reaction cross-sections are summed over final states and averaged over initial states. Because the rapidly varying parts of the cross-section (with energy) are thus filtered out, the S-factor is a slowly varying function of center of mass energy, at least for the non-resonant reactions. It is thus much safer to extrapolate $S(E)$ to the energies relevant for astrophysical environments from the laboratory data, which is usually generated at higher energies (due to difficulties of measuring small cross-sections), than directly extrapolating the $\sigma(E)$, which contains the Gamow transmission factor (see Fig. 2). Additionally, in order to relate $\sigma(E)$ and $S(E)$, quantities measured in the laboratory to these relevant quantities in the solar interior, a correction factor f_0 due to the effects of electron screening needs to be taken into account (53).

In the stellar core with a temperature T , reacting particles have many different velocities (energies) according to a Maxwell - Boltzmann distribution :-

$$\phi(v) = 4\pi v^2 \left(\frac{\mu}{2\pi kT} \right)^{3/2} \exp \left[- \frac{\mu v^2}{2kT} \right] \propto E \exp[-E/kT]$$

Nuclear cross-section or the reaction rates which also depend upon the relative velocity (or equivalently the centre of mass energy) therefore need to be averaged over the thermal velocity (energy) distribution. Therefore, the thermally averaged reaction rate per particle pair is:

$$\langle \sigma v \rangle = \int_0^\infty \phi(v) \sigma(v) v dv = \left(\frac{8}{\pi \mu} \right)^{1/2} \frac{1}{(kT)^{3/2}} \int_0^\infty \sigma(E) E \exp(-E/kT) dE$$

The thermally averaged reaction rate per pair is, utilising the astrophysical S-factor and the energy dependence of the Gamow-factor:

$$\langle \sigma v \rangle = \left(\frac{8}{\pi\mu}\right)^{1/2} \frac{1}{(kT)^{3/2}} \int_0^\infty S(E) \exp\left[-\frac{E}{kT} - \frac{b}{\sqrt{E}}\right] dE$$

with $b^2 = E_G = 2\mu(\pi e^2 Z_1 Z_2 / \hbar)^2 = 0.978\mu Z_1^2 Z_2^2$ MeV, E_G being called the Gamow energy. Note that in the expression for the reaction rate above, at low energies, the exponential term $\exp(-b/\sqrt{E}) = \exp(-\sqrt{E_G/E})$ becomes very small whereas at high energies the Maxwell-Boltzmann factor $\exp(-E/kT)$ vanishes. Hence there would be a peak (at energy, say, E_0) of the integrand for the thermally averaged reaction rate per pair (see Fig. 3). The exponential part of the energy integrand can be approximated as:

$$\exp\left[-\frac{E}{kT} - bE^{-1/2}\right] \sim C \exp\left[-\left(\frac{E - E_0}{\Delta/2}\right)^2\right]$$

where

$$C = \exp(-E_0/kT - bE_0^{-1/2}) = \exp(-3E_0/kT) = \exp(-\tau)$$

with

$$E_0 = (bkT/2)^{\frac{2}{3}} = 1.22\text{keV}(Z_1^2 Z_2^2 \mu T_6^2)^{\frac{1}{3}}$$

and

$$\Delta = 4(E_0 kT/3)^{\frac{1}{2}} = 0.75\text{keV}(Z_1^2 Z_2^2 AT_6^5)^{\frac{1}{6}}$$

Since most stellar reactions happen in a fairly narrow band of energies, $S(E)$ will have a nearly constant value over this band averaging to S_0 . With this, the reaction rate per pair of particles, turns out to be:

$$\langle \sigma v \rangle = \left[\frac{8}{\pi\mu(kT)^3}\right]^{1/2} S_0 \int_0^\infty e^{-\tau - 4\left(\frac{E-E_0}{\Delta}\right)^2} dE = 4.5 \times 10^{14} \frac{S_0}{AZ_1 Z_2} \tau^2 e^{-\tau} \text{cm}^3 \text{s}^{-1}$$

Here,

$$\tau = 3E_0/kT = 42.5(Z_1^2 Z_2^2 \mu/T_6)^{\frac{1}{3}}$$

The maximum value of the integrand in the above equation is:

$$I_{\max} = \exp(-\tau)$$

The values of E_0, I_{max}, Δ , etc., apart from the Coulomb barrier for several reactions are tabulated in Table 1 for $T_6 = 15$.

As the nuclear charge increases, the Coulomb barrier increases, and the Gamow peak E_0 also shifts towards higher energies. Note how rapidly the maximum of the integrand I_{max} decreases with the nuclear charge and the Coulomb barriers. The effective width Δ is a geometric mean of E_0 and kT , and $\Delta/2$ is much less rapidly varying between reactions (for $kT \ll E_0$). The rapid variation of I_{max} indicates that of several nuclei present in the stellar core, those nuclear pairs will have the largest reaction rates, which have the smallest Coulomb barrier. The relevant nuclei will be consumed most rapidly at that stage. (Note however that for the p+p reaction, apart from the Coulomb barrier, the strength of the weak force, which transforms a proton to a neutron also comes into play).

When nuclei of the smallest Coulomb barrier are consumed, there is a temporary dip in the nuclear generation rate, and the star contracts gravitationally until the temperature rises to a point where nuclei with the next lowest Coulomb barrier will start burning. At that stage, further contraction is halted. The star therefore goes through well defined stages of different nuclear burning phases in its core at later epochs dictated by the height of the Coulomb barriers of the fuels. Note also from the Table 1, how far E_0 , the effective mean energy of reaction is below the Coulomb barrier at the relevant temperature. The stellar burning is so slow because the reactions are taking place at such a far sub-Coulomb region, and this is why the stars can last so long.

Table 1: Parameters of the thermally averaged reaction rates at $T_6 = 15$.

Reaction	Coulomb Barrier (MeV)	Gamow Peak (E_0) (keV)	I_{max} ($e^{-3E_0/kT}$)	Δ (keV)	$(\Delta)I_{max}$
p + p	0.55	5.9	1.1×10^{-6}	6.4	7×10^{-6}
p + N	2.27	26.5	1.8×10^{-27}	13.6	2.5×10^{-26}
$\alpha + C^{12}$	3.43	56	3×10^{-57}	19.4	5.9×10^{-56}
$O^{16} + O^{16}$	14.07	237	6.2×10^{-239}	40.4	2.5×10^{-237}

The above discussion assumes that a bare nuclear Coulomb potential is seen by the charged projectile. For nuclear reactions measured in the laboratory, the target nuclei are in the form of atoms with electron cloud surrounding the nucleus and giving rise to a screened potential – the total potential then goes to zero outside the atomic radius. The effect of the screening is to reduce the effective height of the Coulomb barrier. Atoms in the stellar interiors are in most cases in highly stripped state, and nuclei are immersed in a sea of free

electrons which tend to cluster near the nucleus. When the stellar density increases, the so called Debye-Huckel radius $R_D = (kT/4\pi e^2 \rho N_A \xi)^{1/2}$, (here: $\xi = \sum_i (Z_i^2 + Z_i) X_i / A_i$) which is a measure of this cluster “radius”, decreases, and the effect of shielding upon the reaction cross-section becomes more important. This shielding effect enhances thermonuclear reactions inside the star. The enhancement factor $f_0 = \exp(0.188 Z_1 Z_2 \xi \rho^{1/2} T_6^{-3/2})$, varies between 1 and 2 for typical densities and compositions (53) but can be large at high densities.

3. Hydrogen burning: the pp chain

The quantitative aspects of the problem of solar energy production with details of known nuclear physics of converting hydrogen into helium was first worked out by von Weizsäcker (1937-38) (60), (61) and Bethe & Critchfield (1938-1939) (11), which made it clear that two different sets of reactions : the p-p chains and the CN cycle can do this conversion. This happens in the core of the star initially (at the “main sequence” stage), and then later in the life of a star in a shell of burning hydrogen around an inert core of He.

In the first generation of stars in the galaxy only the p-p cycle may have operated. In second generation, heavier elements like C, N from the ashes of burning in previous stars are available and they too can act as catalysts to have thermonuclear fusion of hydrogen to helium. [A recent discovery ((20)) of a low-mass star with an iron abundance as low as 1/200,000 of the solar value (compare the previous record of lowest iron abundance less than 1/10,000 that of the sun), suggests that such first generation stars are still around].

The sun with a central temperature of 15.6 million degrees, ($T_{6\odot}^c = 15.6$) burns by p-p chains. Slightly more massive star (with central temperature $T_6 \geq 20$) burns H by also the CNO cycle. Davis et al.s’ solar neutrino experiment (23), which in 1968 had only an upper limit of the neutrino flux, itself put a limit of less than 9% of the sun’s energy is produced by the carbon-nitrogen cycle (the more recent upper limit (4) is 7.3%, from an analysis of several solar neutrino experiments, including the Kamland measurements. Note however that for the standard solar model, the actual contribution of CNO cycle to solar luminosity is $\sim 1.5\%$ (6)). In CNO cycle, nuclei such as C, N, O serve as “catalysts” do in a chemical reaction. The pp-chain and the CNO cycle reaction sequences are illustrated in Figs. 4 and 10.

The pp-chain begins with the reaction $p + p \rightarrow d + e^+ + \nu_e$. Bethe and Critchfield (11) showed that weak nuclear reaction is capable of converting a proton into a neutron during the brief encounter of a scattering event. (This reaction overcomes the impasse posed by the instability of ${}^2\text{He}$ in the $p + p \rightarrow {}^2\text{He}$ reaction via the strong or electromagnetic

interactions, and as the next nucleus ${}^3\text{Li}$ reachable via these interactions is also unstable as a final product). Since a hydrogen atom is less massive than a neutron, such a conversion would be endothermic (requiring energy), except for the fact that a neutron in a deuterium nucleus ${}^2\text{D}$ can form a bound state with the proton with a binding energy of 2.224 MeV, – thus making the reaction exothermic with an available kinetic energy of 0.42 MeV. The released positron soon pair annihilates and produces photons which makes the total energy released to be 1.442 MeV.

Because of the low Coulomb barrier, in the p+p reaction ($E_c = 0.55$ MeV), a star like the sun would have consumed all its hydrogen quickly (note the relatively large value of $(\Delta)I_{max}$ in Table 1), were it not slowed down by the weakness of the weak interactions. The calculation of probability of deuteron formation consists of two separate considerations: 1) the penetration of a mutual potential barrier in a collision of two protons in a thermal bath and 2) the probability of the β -decay and positron and neutrino emission. Bethe and Critchfield used the original Fermi theory (point interaction) for the second part, which is adequate for the low energy process.

3.1. Cross-section for deuterium formation

The total Hamiltonian H for the p-p interaction can be written as a sum of nuclear term H_n and a weak-interaction term H_w . As the weak interaction term is small compared to the nuclear term, first order perturbation theory can be applied and Fermi’s “Golden rule”, gives the differential cross-section as:

$$d\sigma = \frac{2\pi\rho(E)}{\hbar v_i} | \langle f | H_w | i \rangle |^2$$

here $\rho(E) = dN/dE$, is the density of final states in the interval dE and v_i is the relative velocity of the incoming particles. For a given volume V , the number of states dn between p and $p+dp$ is:-

$$dN = dn_e dn_\nu = \left(V \frac{4\pi p_e^2 dp_e}{h^3} \right) \left(V \frac{4\pi p_\nu^2 dp_\nu}{h^3} \right)$$

By neglecting the recoil energy of deuterium (since this is much heavier than the outgoing positron in the final state) and neglecting the mass of the electron neutrino, we have: $E = E_e + E_\nu = E_e + cp_\nu$ and $dE = dE_\nu = cp_\nu$, for a given E_e and,

$$\rho(E) = dN(E)/dE = dn_e(dn_\nu/dE) = 16\pi^2 V^2 / (c^3 h^6) p_e^2 (E - E_e)^2 dp_e = \rho(E_e) dp_e$$

The matrix element that appears in the differential cross section, may be written in terms of the initial state wave function Ψ_i of the two protons in the entrance channel and the final state wave function Ψ_f as:

$$H_{if} = \int [\Psi_d \Psi_e \Psi_\nu]^* H_\beta \Psi_i d\tau$$

If the energy of the electron is large compared to $Z \times \text{Rydberg}$ (Rydberg $R_\infty = 2\pi^2 m e^4 / ch^3$), then a plane wave approximation is a good one: $\Psi_e = 1/(\sqrt{V}) \exp(i\mathbf{k}_e \cdot \vec{r})$ where the wavefunction is normalised over volume V . (For lower energies, typically 200 keV or less, the electron wave-function could be strongly affected by nuclear charge (see (51)). Apart from this, the final state wave function: $[\Psi_d \Psi_e \Psi_\nu]$ has a deuteron part Ψ_d whose radial part rapidly vanishes outside the nuclear domain (R_0), so that the integration need not extend much beyond $r \simeq R_0$ (for example, the deuteron radius $R_d = 1.7$ fm). Note that because of the Q-value of 0.42 MeV for the reaction, the kinetic energy of the electron ($K_e \leq 0.42$ MeV) and the average energy of the neutrinos ($\bar{E}_\nu = 0.26$ MeV) are low enough so that for both electrons and neutrino wavefunctions, the product $kR_0 \leq 2.2 \times 10^{-3}$ and the exponential can be approximated by the first term of the Taylor expansion:

$$\Psi_e = 1/(\sqrt{V}) [1 + i(\mathbf{k}_e \cdot \vec{r})] \sim 1/(\sqrt{V})$$

and

$$\Psi_\nu \sim 1/(\sqrt{V})$$

Then the expectation value of the Hamiltonian, given a strength of interaction governed by coupling constant g is:

$$H_{if} = \int [\Psi_d \Psi_e \Psi_\nu]^* H_\beta \Psi_i d\tau = \frac{g}{V} \int [\Psi_d]^* \Psi_i d\tau$$

The integration over $d\tau$ can be broken into a space part M_{space} and a spin part M_{spin} , so that the differential cross-section is:

$$d\sigma = \frac{2\pi}{\hbar v_i} \frac{16\pi^2}{c^3 \hbar^6} g^2 M_{spin}^2 M_{space}^2 p_e^2 (E - E_e)^2 dp_e$$

Thus the total cross-section upto an electron energy of E can be obtained by integration as proportional to:

$$\int_0^E p_e^2 (E - E_e)^2 dp_e = \frac{(m_e c^2)^5}{c^3} \int_1^W (W_e^2 - 1)^{1/2} (W - W_e)^2 W_e dW_e$$

where $W = (E + m_e c^2)/m_e c^2$. The integral over W can be shown as:

$$f(W) = (W^2 - 1)^{1/2} \left[\frac{W^4}{30} - \frac{3W^2}{20} - \frac{2}{15} \right] + \frac{W}{4} \ln[W + (W^2 - 1)^{1/2}]$$

so that:

$$\sigma = \frac{m_e^5 c^4}{2\pi^3 \hbar^7} f(W) g^2 M_{space}^2 M_{spin}^2$$

At large energies, the factor $f(W)$ behaves as:

$$f(W) \propto W^5 \propto \frac{1}{30} E^5$$

The process that we are considering: $p + p \rightarrow d + e^+ + \nu_e$, the final state nucleus (deuterium in its ground state) has $J_f^\pi = 1^+$, with a predominant relative orbital angular momentum $l_f = 0$ and $S_f = 1$ (triplet S-state). For a maximum probability of the process, called the super-allowed transition, there are no changes in the *orbital* angular momentum between the initial and final states of the nuclei. Hence for super-allowed transitions, the initial two interacting protons in the $p + p$ reaction that we are considering must have $l_i = 0$. Since the two protons are identical particles, Pauli principle requires $S_i = 0$, so that the total wavefunction will be antisymmetric in space and spin coordinates. Thus, we have a process:

$$|S_i = 0, l_i = 0 \rangle \rightarrow |S_f = 1, l_f = 0 \rangle$$

This is a pure Gamow-Teller⁷ transition with coupling constant $g = C_A$ (due to the axial vector component which can be obtained, for example, in the pure GT transitions of ${}^6\text{He}(0^+) \rightarrow {}^6\text{Li}(1^+)$ decay).

⁷In the beta-decay *allowed* approximation, where we neglect the variation of the lepton wavefunctions and the nuclear momentum over the nuclear volume (this is equivalent to neglecting all total lepton orbital angular momenta $L > 0$) the total angular momentum is carried off by the lepton is just their total spin: i.e. $S = 1$ or 0 , since each lepton has spin $\frac{1}{2}$. When spins of the leptons in the final state are antiparallel, $s_e + s_\nu = s_{tot} = 0$ the process is the Fermi transition with Vector coupling constant $g = C_V$ (example of a pure Fermi decay: ${}^{14}\text{O}(J_i^\pi = 0^+) \rightarrow {}^{14}\text{N}(J_f^\pi = 0^+)$). When the final state lepton spins are parallel, $s_e + s_\nu = s_{tot} = 1$, the process is Gamow-Teller with $g = C_A$. Thus, for the Fermi coupling, there is no change in the (total) angular momentum between the initial and final states of the nuclei ($\Delta J = 0$). For the Gamow-Teller coupling, the selection rules are: $\Delta J = 0$ or ± 1 (but the possibility $\Delta J = 0$ cannot proceed in this case between two states of zero angular momentum). The size of the matrix element for a transition

The spin matrix element in the above expression for energy integrated cross-section σ , is obtained from summing over the final states and averaging over the initial states *and* dividing by 2 to take into account that we have two identical particles in the initial state. Thus,

$$\lambda = \frac{1}{\tau} = \frac{m^5 c^4}{2\pi^3 \hbar^7 v_i} f(W) g^2 \frac{M_{space}^2 M_{spin}^2}{2}$$

where, $M_{spin}^2 = \frac{(2J+1)}{(2J_1+1)(2J_2+1)} = 3$. And the space matrix element is:

$$M_{space} = \int_0^\infty \chi_f(r) \chi_i(r) r^2 dr$$

in units of $\text{cm}^{3/2}$. The above integral contains the radial parts of the nuclear wavefunctions $\chi(r)$, and involves Coulomb wavefunctions for barrier penetration at (low) stellar energies. The integral has been evaluated by numerical methods ((28)), and Fig. 5 shows schematically how the M_{space} is evaluated for the overlap of the deuterium ground state wavefunction with the initial pair of protons state. (See also (54), (7) for details of calculations of the overlap integral and writing the astrophysical S-factor in terms the beta decay rate of the neutron (54) which takes into account of radiative corrections to the axial-vector part of the neutron decay through an effective matrix element, the assumption being that these are the same as that for the proton beta decay in the pp reaction above). In the overlap integral one needs only the S-wave part for the wavefunction of the deuteron ψ_d , as the D-wave part makes no contribution to the matrix element (28), although its contribution to the normalisation has

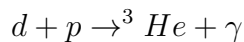
depends essentially on the overlap of the wavefunctions in the initial and final states. In the case of “mirror pair” of nuclei (the nucleus $A_Z = (2Z + 1)_Z$ is the mirror of the nucleus $(2Z + 1)_{Z+1}$), the wavefunctions are very much alike as can be shown through simple heuristic arguments ((25)). For these nuclei, typical ft -values range from $\sim 1000 - 5000$ and are called super-allowed transitions. For super-allowed transitions, which have maximum decay probabilities, there are no changes in the *orbital* angular momentum between the initial and final states of the nuclei. In the $p + p \rightarrow D + e^+ + \nu_e$ reaction, the initial proton state is antisymmetric to an interchange of space and spin coordinates and the final deuteron is symmetric in this respect (in fact when the two protons are in the S state (which is most favourable for their coming together), their spins will be antiparallel (a singlet state) whereas the ground state of the deuteron is a triplet S state. If this were the complete description of the exchange symmetry properties of the Gamow-Teller transition (permitting a change of spin direction of the proton as it transforms to a neutron, changing the total spin by one unit) advocated here this would actually be forbidden. However in the use of configuration space in beta-decay process one must include isotopic spin as well. The 1S state of the two protons is symmetric to exchange of this coordinate, whereas the deuteron (consisting of both a proton and a neutron) function is antisymmetric in this coordinate. In the complete coordinate system the transition is from an initial antisymmetric state to another antisymmetric final state accompanied by a positron emission ((12)).

to be accounted for. The wavefunction of the initial two-proton system ψ_p is normalised to a plane wave of unit amplitude, and again only the S-wave part is needed. The asymptotic form of ψ_p (well outside the range of nuclear forces) is given in terms of regular and irregular Coulomb functions and has to be defined through quantities related to the S-wave phase shifts in p-p scattering data). The result is a miniscule total cross-section of $\sigma = 10^{-47} \text{cm}^2$ at a laboratory beam energy of $E_p = 1 \text{ MeV}$, which cannot be measured experimentally even with milliamperere beam currents.

The reaction $p + p \rightarrow d + e^+ + \nu_e$ is a nonresonant reaction and at all energies the rate varies smoothly with energy (and with stellar temperatures), with $S(0) = 3.8 \times 10^{-22} \text{ keV barn}$ and $dS(0)/dE = 4.2 \times 10^{-24} \text{ barn}$. At for example, the central temperature of the sun $T_6 = 15$, this gives: $\langle \sigma v \rangle_{pp} = 1.2 \times 10^{-43} \text{ cm}^3 \text{ s}^{-1}$ For density in the centre of the sun $\rho = 100 \text{ gm cm}^{-3}$ and an equal mixture of hydrogen and helium ($X_H = X_{He} = 0.5$), the mean life of a hydrogen nucleus against conversion to deuterium is $\tau_H(H) = 1/N_H \langle \sigma v \rangle_{pp} \sim 10^{10} \text{ yr}$. This is comparable to the age of the old stars. The reaction is so slow primarily because of weak interactions and to a lesser extent due to the smallness of the Coulomb barrier penetration factor (which contributes a factor $\sim 10^{-2}$ in the rate), and is the primary reason why stars consume their nuclear fuel of hydrogen so slowly.

3.2. Deuterium burning

Once deuterium is produced in the weak interaction mediated p + p reaction, the main way this is burnt in the sun turns out to be:



This is a nonresonant direct capture reaction to the ${}^3\text{He}$ ground state with a Q-value of 5.497 MeV and $S(0) = 2.5 \times 10^{-3} \text{ keV barn}$. The angle averaged cross-sections measured as a function of proton + deuterium centre of mass energy, where the capture transitions were observed in gamma-ray detectors at several angles to the incident proton beam direction, are well explained by the direct capture model (see Fig. 6 after (49)).

The reactions comprising the rest of the (three) pp-chains start out with the predominant product of deuterium burning: ${}^3\text{He}$ (manufactured from $d + p$ reaction) as the starting point. The only other reactions with a $S(0)$ greater than the above are: $d(d, p)t$, $d(d, n){}^3\text{He}$, $d({}^3\text{He}, p){}^4\text{He}$, and $d({}^3\text{He}, \gamma){}^5\text{Li}$. However, because of the overwhelmingly large number of protons in the stellar thermonuclear reactors, the process involving protons on deuterium dominates.

The rate of this reaction is so fast compared to its precursor: $p + p \rightarrow d + e^+ \nu_e$, that the overall rate of the pp-chain is not determined by this reaction.

One can show that the abundance ratio of deuterium to hydrogen in a quasi-equilibrium has an extremely small value, signifying that deuterium is destroyed in thermonuclear burning. The time dependence of deuterium abundance D is:

$$\frac{dD}{dt} = r_{pp} - r_{pd} = \frac{H^2}{2} \langle \sigma v \rangle_{pp} - HD \langle \sigma v \rangle_{pd}$$

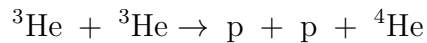
The self regulating system eventually reaches a state of quasi-equilibrium and has:

$$(D/H) = \langle \sigma v \rangle_{pp} / (2 \langle \sigma v \rangle_{pd}) = 5.6 \times 10^{-18}$$

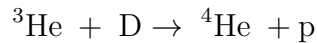
at $T_6 = 5$ and 1.7×10^{-18} at $T_6 = 40$. For the solar system however, this ratio is 1.5×10^{-4} and the observed $(D/H)_{obs}$ ratio in the cosmos is $\sim 10^{-5}$. The higher cosmic ratio is due to primordial nucleosynthesis in the early phase of the universe before the stars formed. (The primordial deuterium abundance is a key quantity used to determine the baryon density in the universe). Stars only destroy the deuterium in their core due to the above reaction.

3.3. ^3He burning

The pp-chain-I is completed (see Fig. 4) through the burning of ^3He via the reaction:



with an S-factor: $S(0) = 5500$ keV barn and Q-value = 12.86 MeV. In addition, the reaction:



has an S-factor: $S(0) = 6240$ keV barn, but since the deuterium concentration is very small as argued above, the first reaction dominates the destruction of ^3He even though both reactions have comparable $S(0)$ factors.

^3He can also be consumed by reactions with ^4He (the latter is pre-existing from the gas cloud from which the star formed and is synthesised in the early universe and in Pop III objects). These reactions proceed through Direct Captures and lead to the ppII and ppIII parts of the chain (happening 15% of the time). Note that the reaction $^3\text{He}(\alpha, \gamma)^7\text{Be}$ together with the subsequent reaction: $^7\text{Be}(p, \gamma)^8\text{B}$ control the production of high energy

neutrinos in the sun and are particularly important for the ^{37}Cl solar neutrino detector constructed by Ray Davis and collaborators.

3.4. Reactions involving ^7Be

As shown in Fig. 4, about 15% of the time, ^3He is burned with ^4He radiatively to ^7Be . Subsequent reactions involving ^7Be as a first step in alternate ways complete the fusion process: $4\text{H} \rightarrow ^4\text{He}$ in the ppII and ppIII chains.

3.4.1. Electron capture process

The first step of the ppII chain is the electron capture reaction on ^7Be : $^7\text{Be} + e^- \rightarrow ^7\text{Li} + \nu_e$ (see Fig 7). This decay goes both to the ground state of ^7Li as well as to its first excited state at $E_X = 0.478$ keV, $J^\pi = \frac{1}{2}^-$) – the percentage of decays to the excited state being 10.4 % in the laboratory. The energy released in the reaction with a Q-value of 0.862 keV is carried away by escaping monoenergetic neutrinos with energies: $E_\nu = 862$ and 384 keV. The measured laboratory mean life of the decay is $\tau = 76.9\text{d}$. The capture rate in the laboratory can be obtained from Fermi’s Golden Rule and utilising the fact that the wavefunctions of both the initial nucleus and the final one vanish rapidly outside the nuclear domain and the electron wavefunction in that domain can be approximated as its value at $r = 0$ and the neutrino wavefunction by a plane wave normalised to volume V, so that $H_{if} = \Psi_e(0)g/\sqrt{V} \int \Psi_{^7\text{Li}}^* \Psi_{^7\text{Be}} d\tau = \Psi_e(0)gM_n/\sqrt{V}$, where M_n represents the nuclear matrix element and the resultant capture rate is:

$$\lambda_{EC} = 1/\tau_{EC} = (g^2 M_n^2 / \pi c^3 \hbar^4) E_\nu^2 |\Psi_e(0)|^2$$

In the laboratory capture process, any of the various electron shells contribute to the capture rate; however the K-shell gives the dominant contribution. At temperatures inside the sun, e.g. $T_6 = 15$, nuclei such as ^7Be are largely ionised. The nuclei however are immersed in a sea of free electrons resulting from the ionised process and therefore electron capture from continuum states is possible (see e.g., (9), (8)). Since all factors in the capture of continuum electrons in the sun are approximately the same as those in the case of atomic electron capture, except for the respective electron densities, the ^7Be lifetime in a star, τ_s is related to the terrestrial lifetime τ_t by:

$$\frac{\tau_{fr}}{\tau_t} \sim \frac{2|\Psi_t(0)|^2}{|\Psi_{fr}(0)|^2}$$

where $|\Psi_{fr}(0)|^2$ is the density of the free electrons $n_e = \rho/m_H$ at the nucleus, ρ being the stellar density. The factor of 2 in the denominator takes care of the two spin states of calculation of the λ_t whereas the corresponding λ_{fr} is calculated by averaging over these two orientations. Taking account of distortions of the electron wavefunctions due to the thermally averaged Coulomb interaction with nuclei of charge Z and contribution due to hydrogen (of mass fraction X_H) and heavier nuclei, one gets the continuum capture rate as:

$$\tau_{fr} = \frac{2|\Psi_t(0)|^2\tau_t}{(\rho/M_H)[(1 + X_H)/2]2\pi Z\alpha(m_e c^2/3kT)^{1/2}}$$

with $|\Psi_e(0)|^2 \sim (Z/a_0)^3/\pi$. Bahcall et al (7) obtained for the 7Be nucleus a lifetime:

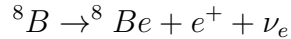
$$\tau_{fr}({}^7Be) = 4.72 \times 10^8 \frac{T_6^{1/2}}{\rho(1 + X_H)} \text{s}$$

The temperature dependence comes from the nuclear Coulomb field corrections to the electron wavefunction which are thermally averaged. For solar condition the above rate (8) gives a continuum capture rate of $\tau_{fr}({}^7Be) = 140d$ as compared to the terrestrial mean life of $\tau_t = 76.9d$. Actually, under stellar conditions, there is a partial contribution from some 7Be atoms which are only partially ionised, leaving electrons in the inner K-shell. So the contributions of such partially ionised atoms have to be taken into account. Under solar conditions the K-shell electrons from partially ionised atoms give another 21% increase in the total decay rate. Including this, gives the solar lifetime of a 7Be nucleus as: $\tau_{\odot}({}^7Be) = 120d$. In addition, the solar fusion reactions have to be corrected for plasma electrostatic screening enhancement effects. For a recent discussion of the issues see (5).

3.4.2. Capture reaction leading to 8B

Apart from the electron capture reaction, the 7Be that is produced is partly consumed by proton capture via: ${}^7Be(p, \alpha){}^8B$ reaction. Under solar conditions, this reaction happens only 0.02% of the time. The proton capture on 7Be proceeds at energies away from the 640 keV resonance via the direct capture process. Since the product 7Li nucleus emits an intense γ -ray flux of 478 keV, this prevents the direct measurement of the direct capture to ground state γ -ray yield. The process is studied indirectly by either the delayed positron or the breakup of the product 8B nucleus into two alpha particles. This reaction has a weighted average $S(0) = 0.0238 \text{ keVbarn}$ (26).

The product: 8B is a radioactive nucleus that decays with a lifetime $\tau = 1.1$ s:

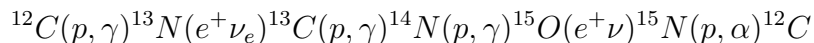


The positron decay of ${}^8B(J^\pi = 2^+)$ goes mainly to the $\Gamma = 1.6$ MeV broad excited state in 8Be at excitation energy $E_x = 2.94$ MeV ($J^\pi = 2^+$) due to the selection rules (see Fig. 8). This excited state has very short lifetime and quickly decays into two α -particles. This completes the ppIII part of the pp-chain. The average energy of the neutrinos from 8B reactions is: $\bar{E}_\nu({}^8B) = 7.3$ MeV. These neutrinos, having relatively high energy, play an important role in several solar neutrino experiments.

4. The CNO cycle and hot CNO

The sun gets most of its energy generation through the pp-chain reactions (see Fig. 9). However, as the central temperature (in stars more massive than the sun) gets higher, the CNO cycle (see below for reaction sequence) comes to dominate over the pp-chain at T_6 near 20 (this changeover assumes the solar CNO abundance, the transition temperature depends upon CNO abundance in the star). The early generation of stars (usually referred to as the Population II (or Pop II stars), although there is an even earlier generation of Pop III stars) generated energy primarily through the pp-chain. These stars are still shining in globular clusters, and being of mass lower than that of the sun, are very old. Most other stars that we see today are later generation stars formed from the debris of heavier stars that contained heavy elements apart from (the most abundant) hydrogen. Thus in the second and third generation stars (which are slightly heavier than the sun) where higher central temperatures are possible because of higher gravity, hydrogen burning can take place through faster chain of reactions involving heavy elements C, N, and O which have some reasonable abundance (exceeding 1%) compared to other heavy elements like Li, Be, B which are extremely low in abundance. The favoured reactions involve heavier elements (than those of the pp-chain) which have the smallest Coulomb barriers but with reasonably high abundance. Even though the Coulomb barriers of Li, Be, B are smaller than those of C, N, O (when protons are the lighter reactants (projectiles)), they lose out due to their lower abundance.

In 1937-1938, Bethe and von Weizsäcker independently suggested the CN part of the cycle, which goes as:



This has the net result, as before: $4p \rightarrow {}^4He + 2e^+ + 2\nu_e$ with a $Q = 26.73$. In these

reactions, the ^{12}C and ^{14}N act merely as catalysts as their nuclei are “returned” at the end of the cycle. Therefore the ^{12}C nuclei act as seeds that can be used over and over again, even though the abundance of the seed material is miniscule compared to the hydrogen. But note that there is a loss of the catalytic material from the CN cycle that takes place through the $^{15}\text{N}(p, \gamma)^{16}\text{O}$ reactions. However, the catalytic material is subsequently returned to the CN cycle by the reaction: $^{16}\text{O}(p, \gamma)^{17}\text{F}(e^+\nu_e)^{17}\text{O}(p, \alpha)^{14}\text{N}$.

In the CN cycle (see Fig 10), the two neutrinos involved in the beta decays (of ^{13}N ($t_{1/2} = 9.97\text{min}$) and ^{15}O ($t_{1/2} = 122.24\text{s}$)) are of relatively low energy and most of the total energy $Q = 26.73$ MeV from the conversion of four protons into helium is deposited in the stellar thermonuclear reactor. The rate of the energy production is governed by the slowest thermonuclear reaction in the cycle. Here nitrogen isotopes have the highest Coulomb barriers in charged particle reactions, because of their $Z = 7$. Among them $^{14}\text{N}(p, \gamma)^{15}\text{O}$ is the slowest because this reaction having a final state photon is governed by electromagnetic forces while that involving the other nitrogen isotope: $^{15}\text{N}(p, \alpha)^{12}\text{C}$ is governed by strong forces and is therefore faster.

From the CN cycle, there is actually a branching off from ^{15}N by the reaction $^{15}\text{N}(p, \gamma)^{16}\text{O}$ mentioned above. This involves isotopes of oxygen, and is called the ON cycle; finally the nitrogen is returned to the CN cycle through ^{14}N . Together the CN and the ON cycles, constitutes the CNO bi-cycle. The two cycles differ considerably in their relative cycle-rates: the ON cycle operates only once for every 1000 cycles of the main CN cycle. This can be gauged from the $S(0)$ factors of the two sets of reactions branching off from ^{15}N : for the $^{15}\text{N}(p, \alpha)^{12}\text{C}$ reaction $S(0) = 65$ MeV b, whereas for $^{15}\text{N}(p, \gamma)^{16}\text{O}$, it is 64 keV b, i.e. a factor of 1000 smaller.

4.1. Hot CNO and rp-process

The above discussion of CNO cycle is relevant for typical temperatures $T_6 \geq 20$. These are found in quiescently hydrogen burning stars with solar composition which are only slightly more massive than the sun. There are situations where the hydrogen burning takes place at temperatures ($T \sim 10^8 - 10^9$ K) which are far in excess of those found in the interiors of the ordinary “main sequence” stars. Examples of these are: hydrogen burning at the accreting surface of a neutron star or in the explosive burning on the surface of a white dwarf, i.e. novae, or the outer layers of a supernova shock heated material in the stellar mantle. These hot CNO cycles operate under such conditions on a rapid enough timescale (few seconds) so that even “normally” β -unstable nuclei like ^{13}N will live long enough to be burned by thermonuclear charged particle reactions, before they are able to β -decay. The process of

normal CNO and a typical part of hot CNO (at $T_9 = 0.2$) in the (N,Z) plane is illustrated in Fig. 12. So, unlike the normal CNO the amount of hydrogen to helium conversion in hot CNO is limited by the β -decay lifetimes of the proton-rich nuclei like: ^{14}O and ^{15}O rather than the proton capture rate of ^{14}N . Wallace and Woosley (1981, (58)) has shown that for temperatures, $T \geq 5 \times 10^8 \text{K}$, nucleosynthesised material can leak out of the cycles. This leads to a diversion from lighter to heavier nuclei and is known as the rapid proton capture or rp-process.

The nucleosynthesis path of rp-process of rapid proton addition is analogous to the r-process of neutron addition. The hot hydrogen bath converts CNO nuclei into isotopes near the region of proton unbound nuclei (the proton drip line). For each neutron number, a maximum mass number A is reached where the proton capture must wait until β^+ -decay takes place before the buildup of heavier nuclei (for an increased neutron number) can take place. Unlike the r-process the rate of the rp-process is increasingly hindered due to the increasing Coulomb barrier of heavier and higher-Z nuclei to proton projectiles. Thus the rp-process does not extend all the way to the proton drip line but runs close to the beta-stability valley and runs through where the β^+ -decay rate compares favourably with the proton captures. A comparison of the reaction paths of rp- and r-processes in the (N,Z) plane is given in Fig. 13. A useful web reference for the rp-process in a nutshell is Guidry (1994) (30) (see also (59), (63)).

5. Helium burning and the triple- α reaction

After hydrogen burning in the core of the star has exhausted its fuel, the helium core contracts slowly. Its density and temperature goes up as gravitational energy released is converted to internal kinetic energy. The contraction also heats hydrogen at the edge of the helium core, igniting the hydrogen to burn in a shell. At a still later stage in the star's evolution, the core has contracted enough to reach central temperature density conditions: $T_6 = 100 - 200$ and $\rho_c = 10^2 - 10^5 \text{ gm cm}^{-3}$ when the stellar core settles down to burn ^4He in a stable manner. The product of helium burning is ^{12}C . Since in nature, the $A = 5$ and $A = 8$ nuclei are not stable, the question arises as to how helium burning bridges this gap. A direct interaction of three α particles to produce a ^{12}C nucleus would seem at first sight, to be too improbable (as was mentioned, for example, in Bethe's 1939 paper (13), which was primarily on the CN cycle). However, Öpik (43) and Salpeter (54), (52) independently proposed a two step process where in the first step, two α particles interact to produce a ^8Be nucleus in its ground state (which is unstable to α -breakup), followed by the unstable nucleus interacting with another α -particle process to produce a ^{12}C nucleus.

Thus the triple alpha reaction begins with the formation of ${}^8\text{Be}$ that has a lifetime of only 1×10^{-16} s (this is found from the width $\Gamma = 6.8$ eV of the ground state and is the cause of the $A = 8$ mass gap). This is however long compared to the transit time 1×10^{-19} s of two α -particles to scatter past each other non-resonantly with kinetic energies comparable to the Q -value of the reaction namely, $Q = -92.1$ keV. So it is possible to have an equilibrium build-up of a small quantity of ${}^8\text{Be}$ in equilibrium with its decay or reaction products: $\alpha + \alpha \rightarrow {}^8\text{Be}$. The equilibrium concentration of the ${}^8\text{Be}$ nucleus can be calculated through the Saha equation

$$N_{12} = \frac{N_1 N_2}{2} \left(\frac{2\pi}{\mu kT} \right)^{3/2} \hbar^3 \frac{(2J+1)}{(2J_1+1)(2J_2+1)} \exp\left(-\frac{E_R}{kT}\right)$$

at the relevant temperature $T_6 = 11$ and $\rho = 10^5$ gm cm $^{-3}$ to be:

$$\frac{N({}^8\text{Be})}{N({}^4\text{He})} = 5.2 \times 10^{-10}$$

Salpeter suggested that this small quantity of ${}^8\text{Be}$ serves as the seed for the second stage of the triple α -capture into the ${}^{12}\text{C}$ nucleus. It was however shown by Hoyle (36) that the amount of ${}^{12}\text{C}$ produced for the conditions inside a star at the tip of the red-giant branch is insufficient to explain the observed abundance, *unless* the reaction proceeds through a resonance process (35). The presence of such a resonance greatly speeds up the rate of the triple- α process which then proceeds through an s-wave ($l = 0$) resonance in ${}^{12}\text{C}$ near the threshold of ${}^8\text{Be} + \alpha$ reaction. Since ${}^8\text{Be}$ and ${}^4\text{He}$ both have $J^\pi = 0^+$, an s-wave resonance would imply that the resonant state in question has to be 0^+ in the ${}^{12}\text{C}$ nucleus. Hoyle suggested the excitation energy to be: $E_X \sim 7.68$ MeV in the ${}^{12}\text{C}$ nucleus and this state was experimentally found by W.A. Fowler's group ((22)) with spin-parity: $J^\pi = 0^+$. This state has a total width ((49)) $\Gamma = 8.9 \pm 1.08$ eV, most of which lies in Γ_α , due to the major propensity of the ${}^{12}\text{C}$ nucleus to break-up through α -decay. (The decay of the excited state of ${}^{12}\text{C}$ by γ -rays cannot go directly to the ground state, since the resonance state as well as the ground state of the ${}^{12}\text{C}$ nucleus have both $J^\pi = 0^+$ and $0^+ \rightarrow 0^+$ decays are forbidden. This partial width due to gamma-decay is several thousand times smaller than that due to α -decay). So, $\Gamma = \Gamma_\alpha + \Gamma_{rad} \sim \Gamma_\alpha$ and $\Gamma_{rad} = \Gamma_\gamma + \Gamma_{e^+e^-} = 3.67 \pm 0.50$ meV. Again the radiative width Γ_{rad} is dominated by the width due to photon width deexcitation: $\Gamma_\gamma = 3.58 \pm 0.46$ meV. (Note the scales of *millielectron* Volts). The reaction scheme for the first and the second parts of the triple-alpha reaction is given in Fig. 14. The locations of the Gamow energy regions near the above resonance state (for several stellar temperatures) are shown only schematically.

The reaction rate for the ${}^{12}\text{C}$ formation can be calculated by using the properties of the

resonant state and the thermally averaged cross-section:

$$r_{3\alpha} = N_{8Be} N_{\alpha} \langle \sigma v \rangle_{8Be+\alpha}$$

Here N_{8Be} and N_{α} are the number densities of interacting 8Be and 4He nuclei and the angular brackets denote thermal averaging over a Maxwell Boltzmann distribution $\psi(E)$. This averaging leads to:

$$r_{3\alpha} = N_{8Be} N_{\alpha} \int_0^{\infty} \psi(E) v(E) \sigma(E) dE$$

with

$$\psi(E) = \frac{2}{\sqrt{\pi}} \frac{E}{kT} \exp(-E/kT) \frac{dE}{(kTE)^{1/2}}$$

and

$$\sigma(E) = \pi \left(\frac{\lambda}{2\pi} \right)^2 \frac{2J+1}{(2J_1+1)(2J_2+1)} \frac{\Gamma_1 \Gamma_2}{(E - E_R)^2 + (\Gamma/2)^2}$$

is the Breit-Wigner resonant reaction cross section with the resonant energy centroid at $E = E_R$. The total width Γ is a sum of all decay channel widths such as $\Gamma_1 = \Gamma_{\alpha}$ and $\Gamma_2 = \Gamma_{\gamma}$. If the width Γ is only a few eVs then the functions $\psi(E)$ and $v(E)$ can be pulled out of the integral. Then, the reaction rate will contain an integral like: $\int_0^{\infty} \sigma_{BW}(E) dE = 2\pi(\lambda/2\pi\hbar)^2 \omega \Gamma_1 \Gamma_2 / \Gamma$, where $\omega = (2J+1)/[(2J_1+1)(2J_2+1)]$ and the functions pulled out of the integral need to be evaluated at $E = E_R$. Since most of the time the excited state of the ${}^{12}C^*$ breaks-up into α -particles, we have $\Gamma_1 = \Gamma_{\alpha}$ dominating over Γ_{γ} and $(\Gamma_1 \Gamma_2 / \Gamma) \sim \Gamma_2$. This limit usually holds for resonances of energy sufficiently high so that the incident particle width (Γ_1) to dominate the natural width of the state (Γ_2). In that case, we can use the number density of the 8Be nuclei in equilibrium with the α -particle nuclei bath as described by Saha equilibrium condition:

$$N({}^8Be) = N_{\alpha}^2 \omega f \frac{h^3}{(2\pi\mu kT)^{3/2}} \exp(-E_r/kT)$$

where f is the screening factor. It is possible to get the overall triple-alpha reaction rate by calculating the equilibrium concentration of the excited (resonant) state of ${}^{12}C$ reached by the ${}^8Be + \alpha \rightarrow {}^{12}C^*$ reaction and then multiplying that concentration by the gamma-decay rate Γ_{γ}/\hbar which leads to the final product of ${}^{12}C$. So, the reaction rate for the final step of the triple-alpha reaction turns out to be:

$$r_{3\alpha} = N_{8Be} N_{\alpha} \hbar^2 \left(\frac{2\pi}{\mu kT} \right)^{3/2} \omega f \Gamma_2 \exp(-E'_r/kT)$$

where μ is the reduced mass of the reactants ${}^8\text{Be}$ and α particle. This further reduces by the above argument to:

$$r_{3\alpha \rightarrow {}^{12}\text{C}} = \frac{N_\alpha^3}{2} 3^{3/2} \left(\frac{2\pi\hbar^2}{M_\alpha kT} \right)^3 f \frac{\Gamma_\alpha \Gamma_\gamma}{\Gamma \hbar} \exp(-Q/kT)$$

The Q -value of the reaction is the sum of $E_R({}^8\text{Be} + \alpha) = 287$ keV and $E_R(\alpha + \alpha) = |Q| = 92$ keV and turns out to be: $Q_{3\alpha} = (M_{{}^{12}\text{C}^*} - 3M_\alpha)c^2 = 379.38 \pm 0.20$ keV ((42)). Numerically, the energy generation rate for the triple-alpha reaction is:

$$\epsilon_{3\alpha} = \frac{r_{3\alpha} Q_{3\alpha}}{\rho} = 3.9 \times 10^{11} \frac{\rho^2 X_\alpha^3}{T_8^3} f \exp(-42.94/T_8) \text{ erg gm}^{-1} \text{ s}^{-1}$$

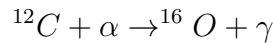
The triple alpha reaction has a very strong temperature dependence: near a value of temperature T_0 , one can show that the energy generation rate is:

$$\epsilon(T) = \epsilon(T_0) \left(\frac{T}{T_0} \right)^n$$

where, $n = 42.9/T_8 - 3$. Thus at a sufficiently high temperature and density, the helium gas is very highly explosive, so that a small temperature rise gives rise to greatly accelerated reaction rate and energy liberation. When helium thermonuclear burning is ignited in the stellar core under degenerate conditions, an unstable and sometimes an explosive condition develops.

6. Survival of ${}^{12}\text{C}$ in red giant stars and ${}^{12}\text{C}(\alpha, \gamma){}^{16}\text{O}$ reaction

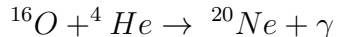
The product of the triple-alpha reactions, ${}^{12}\text{C}$ is burned into ${}^{16}\text{O}$ by α -capture reactions:



If this reaction proceeds too efficiently, then all the carbon will be burned up to oxygen. Carbon is however the most abundant element in the universe after hydrogen, helium and oxygen, and the cosmic C/O ratio is about 0.6. In fact, the O and C burning reactions and the conversion of He into C and O take place in similar stellar core temperature and density conditions. Major ashes of He burning in Red Giant stars are C and O. Red Giants are the source of the galactic supply of ${}^{12}\text{C}$ and ${}^{16}\text{O}$. Fortuitous circumstances of the energy level structures of these alpha-particle nuclei are in fact important for the observed abundance of oxygen and carbon.

For example, if as in the case of the 3α reaction, there was a resonance in the $^{12}\text{C}(\alpha, \gamma)^{16}\text{O}$ reaction near the Gamow window for He burning conditions (i.e. $T_9 \sim 0.1 - 0.2$), then the conversion of $^{12}\text{C} \rightarrow ^{16}\text{O}$ would have proceeded at a very rapid rate. However, the energy level diagram of ^{16}O shows that for temperatures upto about $T_9 \sim 2$, there is no level available in ^{16}O to foster a resonant reaction behaviour (Fig. 15). But since this nucleus is found in nature, its production must go through either: 1) a non-resonant direct capture reaction or 2) nonresonant captures into the tails of nearby resonances (i.e. subthreshold reactions). In Fig. 15, also shown on the left of the ^{16}O energy levels, is the threshold for the $^{12}\text{C} + ^4\text{He}$ reaction, drawn at the appropriate level with respect to the ground state of the ^{16}O nucleus. The Gamow energy regions drawn on the extreme right for temperatures $T_9 = 0.1$ and above, indicates that for the expected central temperatures, the effective stellar (centre of mass) energy region is near $E_0 = 0.3$ MeV. This energy region is reached by the low energy tail of a broad resonance centred at $E_{CM} = 2.42$ MeV above the threshold (the $J^\pi = 1^-$ state at 9.58 MeV above the ground state of ^{16}O) with a (relatively large) resonance width of 400 keV. On the other hand, there are two subthreshold resonances in ^{16}O (at $E_X = 7.12$ MeV and $E_X = 6.92$ MeV), i.e. -45 keV and -245 keV *below* the α -particle threshold that have $J^\pi = 1^-$ and $J^\pi = 2^+$, that contribute to stellar burning rate by their high energy tails. However, electric dipole (E1) γ -decay of the 7.12 MeV state is inhibited by isospin selection rules. Had this not been the case, the $^{12}\text{C}(\alpha, \gamma)^{16}\text{O}$ reaction would have proceeded fast and ^{12}C would have been consumed during helium burning itself. The two subthreshold states at -45 keV and -245 keV give contributions to the astrophysical S-factor of: $S_{1^-}(E_0) = 0.1$ MeV barn and $S_{2^+}(E_0) = 0.2$ MeV barn respectively at the relevant stellar energy $E_0 = 0.3$ MeV. The state at $E_{CM} = 2.42$ MeV ($J^\pi = 1^-$ state at 9.58 MeV) gives a contribution: $S_{1^-}(E_0) = 1.5 \times 10^{-3}$ MeV barn. The total S-factor at $E_0 = 0.3$ MeV is therefore close to 0.3 MeV barn. These then provide low enough S or cross-section to not burn away the ^{12}C entirely to ^{16}O , so that $C/O \sim 0.1$ at the least.

Additionally, ^{16}O nuclei are not burnt away by further α -capture in the reaction:



A look at the level schemes of ^{20}Ne (see Fig. 16) to shows the existence of a $E_X = 4.97$ MeV state ($J^\pi = 2^-$) in the Gamow window. However, this state cannot form in the resonance reaction due to considerations of parity conservation (unnatural parity of the resonant state)⁸. The lower 4.25 MeV state ($J^\pi = 4^+$) in ^{20}Ne also cannot act as a subthreshold resonance

⁸Whether or not a resonant state can be formed or accessed via a given reaction channel depends upon the angular momentum and parity conservation laws. The spins of the particles in the entrance channel, j_1, j_2 and relative angular momentum l adds upto the angular momentum of the resonant state $J = j_1 + j_2 + l$.

as it lies too far below threshold and is formed in the g-wave state. Therefore only direct capture reactions seem to be operative, which for (α, γ) reactions lead to cross-sections in the range of nanobarns or below. Thus the destruction of ^{16}O via: $^{16}\text{O}(\alpha, \gamma)^{20}\text{Ne}$ reaction proceeds at a very slow rate during the stage of helium burning in Red Giant stars, for which the major ashes are carbon and oxygen and these elements have their galactic origin in the Red Giants.

To summarise, the synthesis of two important elements for the evolution of life as we know on the earth have depended upon fortuitous circumstances of nuclear properties and selection rules for nuclear reactions. These are: 1) the mass of the unstable lowest (ground) state of ^8Be being close to the combined mass of two α -particles; 2) there is a resonance in ^{12}C at 7.65 MeV which enhances the alpha addition reaction (the second step); and 3) parity conservation has protected ^{16}O from being destroyed in the $^{16}\text{O}(\alpha, \gamma)^{20}\text{Ne}$ reactions by making the 4.97 MeV excited state in ^{20}Ne of unnatural parity.

7. Advanced stages of thermonuclear burning

As the helium burning progresses, the stellar core is increasingly made up of C and O. At the end of helium burning, all hydrogen and helium is converted into a mixture⁹ of C and O, and since H, He are most abundant elements in the original gas from which the star formed, the amount of C and O are far more than the traces of heavy elements in the gas cloud. Between these two products, the Coulomb barrier for further thermonuclear reaction involving the products is lower for C nuclei. At first the C+O rich core is surrounded by He burning shells and a helium rich layer, which in turn may be surrounded by hydrogen burning shell and the unignited hydrogen rich envelope. When the helium burning ceases to provide sufficient power, the star begins to contract again under its own gravity and as implied by the Virial theorem the temperature of the helium exhausted core rises. The contraction continues until either the next nuclear fuel begins to burn at rapid enough rate

Therefore, for spinless particles like the closed shell nuclei $^4\text{He}, ^{16}\text{O}$ ($j_1 = 0, j_2 = 0$), we have $J = l$. In the entrance channel of the reacting particles, the parity would be: $(-1)^l \pi(j_1) \pi(j_2) = (-1)^{l=0} (1)(1)$. If the parity of the resonance state were the same as that of the entrance channel, then the resultant state would have been a “natural parity” state. However, since the 4.97 MeV state in ^{20}Ne has an assignment: $J^\pi = 2^-$, this is an “unnatural parity” state.

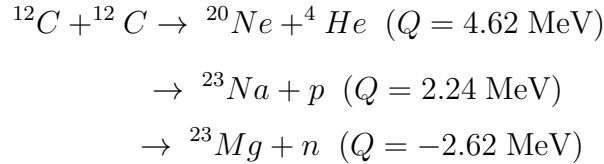
⁹Note however the caveat: if the amount of ^{12}C is little (either due to a long stellar lifetime of He burning or due to a larger rate of the $^{12}\text{C} + \alpha \rightarrow ^{16}\text{O} + \gamma$ reaction whose estimate outlined in the earlier section is somewhat uncertain), then the star may directly go from He-burning stage to the O-burning or Ne-burning stage skipping C-burning altogether ((62)).

or until electron degeneracy pressure halts the infall.

7.1. Carbon burning

Stars somewhat more massive than about $0.7 M_{\odot}$ contract until the temperature is large enough for carbon to interact with itself (stars less massive may settle as degenerate helium white dwarfs). For stars which are more massive than $M \geq 8 - 10 M_{\odot}$ (mass on the main sequence, - *not* the mass of the C+O core), the contracting C+O core remains nondegenerate until C starts burning at $T \sim 5 \times 10^8 K$ and $\rho = 3 \times 10^6 \text{ gcm}^{-3}$. Thereafter sufficient power is generated and the contraction stops and quiescent (hydrostatic, not explosive) C-burning proceeds (see Fig. 17).

The combined mass of two reacting ^{12}C nuclei falls at an excitation energy of 14 MeV in the compound nucleus of ^{24}Mg . At this energy there are many compound nuclear states, and the most effective range of stellar energies (the Gamow window) at the relevant temperature is about 1 MeV; hence a number of resonant states can contribute to the decay of the compound nucleus, and even the large angular momentum resonances may be important because the penetration factors in massive nuclei are not affected by centrifugal barriers. The carbon on carbon burning can proceed through multiple, energetically allowed reaction channels, listed below:



At the temperatures where carbon burning starts, the neutron liberating reactions requires too much particle kinetic energy to be effective. In addition, based on laboratory measurements at higher energies compared to the stellar energies, the electromagnetic decay channel ($^{24}Mg + \gamma$) and the three particle channel ($^{16}O + 2\alpha$) have lower probability compared to the two particle channels: $^{23}Na + p$ and $^{20}Ne + \alpha$. The latter two channels have nearly equal probabilities (see (21); at the lowest centre of mass energies for which cross-sections are measured in the laboratory for the proton and α channels, (i.e. about 2.45 MeV (40)), the branching ratios were $b_p \sim 0.6$ and $b_{\alpha} \sim 0.4$), and therefore the direct products of carbon burning are likely to be ^{23}Na , ^{20}Ne , protons and alpha particles. The rate for this reaction per pair of ^{12}C nuclei is ((48)):

$$\log \lambda_{12,12} = \log f_{12,12} + 4.3 - \frac{36.55(1 + 0.1T_9)^{1/3}}{T_9^{1/3}} - \frac{2}{3} \log T_9$$

the factor $f_{12,12}$ is a screening factor. Now, at the temperatures of ^{12}C burning, the liberated protons and alpha particles can be quickly consumed through the reaction chain: $^{12}\text{C}(p, \gamma)^{13}\text{N}(e^+\nu_e)^{13}\text{C}(\alpha, n)^{16}\text{O}$. Thus, the net effect is that the free proton is converted into a free neutron (which may be further captured) and the α -particle is consumed with ^{12}C into ^{16}O . The α -particles are also captured by other alpha-particle nuclei, resulting in, at the end of carbon burning in nuclei like: ^{16}O , ^{20}Ne , ^{24}Mg and ^{28}Si . These secondary reactions augment the energy released by the initial carbon reaction and Reeves (1959) estimated that each pair of ^{12}C nuclei release about 13 MeV of energy. Towards the end of carbon burning phase there are also other reactions such as: $^{12}\text{C} + ^{16}\text{O}$ and $^{12}\text{C} + ^{20}\text{Ne}$ which take place. But these are less rapid and are not expected to play major roles compared to the $^{12}\text{C} + ^{12}\text{C}$ reactions, due to their increased Coulomb barriers. A recent discussion of the heavy ion reactions involving C and O is contained in (1) section 3.6j

During the carbon-burning and subsequent stages, the dominant energy loss from the star is due to neutrinos streaming out directly from the stellar thermonuclear furnace, rather than by photons from the surface. The neutrino luminosity is a sensitive function of core temperature and quickly outshines the surface photon luminosity of the star at carbon burning stage. The (thermal) evolutionary timescale of the star, due to the neutrino emission becomes very short and the core evolves rapidly, – so rapidly (compared to the “cooling” timescale Kelvin-Helmholtz time: $\tau_{KH} \sim GM^2/RL_{ph}$) that the conditions in the core are “not communicated” to the surface, since this communication happens by photon diffusion. The surface conditions (e.g. the temperature) of the star then does not markedly evolve as the core goes beyond the carbon burning stage, and it may not be possible just by looking at a star’s surface conditions whether the core is close to a supernova stage or has many thousands of years of hydrostatic thermonuclear burning to go.

7.2. Neon burning

The result of carbon burning is mainly neon, sodium and magnesium, but aluminium and silicon are also produced in small quantities by the capture of α , p and n released during carbon burning. When carbon fuel is exhausted, again the core contracts and its temperature T_c goes up. At approximately $T_9 \sim 1$, energetic photons from the high energy tail of the Planck distribution function can begin to disintegrate the ^{20}Ne ash (see Fig. 16) so that one has the reaction: $^{20}\text{Ne} + \gamma \rightarrow ^{16}\text{O} + ^4\text{He}$.

Nucleons in a nucleus are bound with typical binding energy of several to 8 MeV. One would require an energetic γ -ray photon to photo-eject a nucleon. Two nucleon ejection would require more energy. Alpha particles are however released at approximately the same

energy as a nucleon due to the low separation energy of an alpha particle in the nucleus. For example, the alpha separation energy in ^{20}Ne is 4.73 MeV. Thus, the major photonuclear reactions are: (γ, n) , (γ, p) and (γ, α) processes. For a photodisintegration reaction to proceed through an excited state E_X in the mother, the decay rate is:-

$$\lambda(\gamma, \alpha) = \left[\exp\left(-\frac{E_X}{kT}\right) \frac{2J_R + 1}{2J_0 + 1} \frac{\Gamma_\gamma}{\Gamma} \right] \times \frac{\Gamma_\alpha}{\hbar}$$

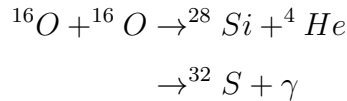
In the above equation, the first factor in square brackets on the RHS is the probability of finding the nucleus in the excited state E_X and spin J_R (with J_0 being the ground state spin), while the second factor Γ_α/\hbar is the decay rate of the excited state with an alpha particle emission. Now since $E_X = E_R + Q$, we have:

$$\lambda(\gamma, \alpha) = \frac{\exp(-Q/kT)}{\hbar(2J_0 + 1)} (2J_R + 1) \frac{\Gamma_\alpha \Gamma_\gamma}{\Gamma} \exp(-E_R/kT)$$

At $T_9 \geq 1$, the photodisintegration is dominated by the 5.63 MeV level in ^{20}Ne (see Fig. 16). At approximately $T_9 \sim 1.5$, the photodissociation rate becomes greater than the rate for alpha capture on ^{16}O to produce ^{20}Ne (i.e. the reverse reaction), thus leading effectively to the net dissociation of ^{20}Ne . The released ^4He reacts with the unspent ^{20}Ne and leads to: $^4\text{He} + ^{20}\text{Ne} \rightarrow ^{24}\text{Mg} + \gamma$. Thus the net result of the photodissociation of two ^{20}Ne nuclei is: $2 \times ^{20}\text{Ne} \rightarrow ^{16}\text{O} + ^{24}\text{Mg}$ with a net Q-value of 4.58 MeV. The brief neon burning phase concludes at T_9 close to ~ 1 .

7.3. Oxygen burning

At the end of the neon burning the core is left with a mixture of alpha particle nuclei: ^{16}O and ^{24}Mg . After this another core contraction phase ensues and the core heats up, until at $T_9 \sim 2$, ^{16}O begins to react with itself:



The first reaction takes place approximately 45% of the time with a Q-value of 9.593 MeV. In addition to Si and S, the oxygen burning phase also produces, Ar, Ca and trace amounts of Cl, K, etc upto Sc. Then at $T_9 \sim 3$, the produced ^{28}Si begins to burn in what is known as the Si burning phase.

7.4. Silicon burning

As we have seen, most of the stages of stellar burning involve thermonuclear fusion of nuclei to produce higher Z and A nuclei. The first exception to this is neon burning where the photon field is sufficiently energetic to photodissociate neon, before the temperature rises sufficiently to allow fusion reactions among oxygen nuclei to overcome their Coulomb repulsion. Processing in the neon burning phase takes place with the addition of helium nuclei to the undissociated neon rather than overcoming the Coulomb barrier of two neon nuclei. This trend continues in the silicon burning phase. In general, a photodisintegration channel becomes important when the temperature rises to the point that the Q -value, i.e. the energy difference between the fuel and the products is smaller than approximately $30k_B T$ ((34)).

With typical Q -values for reactions among stable nuclei above silicon being 8-12 MeV, photodisintegration of the nuclear products of neon and oxygen burning begins to play an important role once the temperature exceeds: $T_9 \geq 3$. Then nuclei with smaller binding energies are destroyed by photodissociation in favour of their more tightly bound neighbours, and many nuclear reactions involving α -particles, protons and neutrons interacting with all the nuclei in the mass range $A = 28 - 65$ take place. In contrast to the previous burning stages where only a few nuclei underwent thermonuclear reactions upon themselves, here the nuclear reactions are primarily of a rearrangement type, in which a particle is photoejected from one nucleus and captured by another and a given fuel nucleus is linked to a product nucleus by a multitude of reaction chains and cycles and it is necessary to keep track of many more nuclei (and many reaction processes involving these) than for previous burning stages.. More and more stable forms of the nuclei form in a nuclear reaction network as the rearrangement proceeds. Since there exists a maximum in the binding energy per nucleon at the ^{56}Fe nucleus, the rearrangements lead to nuclei in the vicinity of this nucleus (i.e. iron-group nuclei).

In the mass range $A = 28 - 65$, the levels in the compound nuclei that form in the reactions during silicon burning are so dense that they overlap. Moreover, at the high temperatures that are involved ($T_9 = 3 - 5$), the net reaction flux may be small compared to the large forward and backward reactions involving a particular nucleus and a quasi-equilibrium may ensue between groups of nuclei which are connected between separate groups by a few, slow, rate-limiting reactions (“bottlenecks”). However, as the available nuclear fuel(s) are consumed and thermal energy is removed due to escaping neutrinos, various nuclear reactions may no longer occur substantially rapidly (“freeze-out”). Thielemann and Arnett ((57)) found that for cores of massive stars in hydrostatic cases, the bottlenecks between quasi-equilibrium (QSE) groups coincided with $Z=21$ nuclei whereas for lower mass

stars, lower temperatures and Y_e and higher density this bridge involved neutron rich isotopes of Ca capturing protons. Hix and Thielemann (34) discussed and contrasted these results with those of earlier workers and in general the reaction flow across the boundary of the QSE groups are influenced by the neutronisation of the material, i.e. the overall Y_e . It is in this context that weak interaction processes such as electron capture and beta decay of nuclei are important, by influencing the Y_e and thereby the reaction flow. These ultimately affect both the stellar core density and entropy structures, and it is important to track and include the changing Y_e of the core material not only in the silicon burning phase, but even from earlier oxygen burning phases. The calculation of stellar weak processes on nuclei has spawned extensive literature (see (29), (37) etc., and (39) for a review).

In summary, a few key points concerning the thermonuclear burning of ^{28}Si are as follows:-

- Direct thermonuclear fusion of two ^{28}Si nuclei does not take place because their Coulomb barrier is too high. Instead thermonuclear fusion takes place by successive additions of α -particles, neutrons and protons.

- Although this is actually a large network of nuclear reactions it is called “silicon burning” because ^{28}Si offers the largest resistance to photo-dissociation because of its highest binding energy among intermediate mass nuclei.

- The source of the α -particles which are captured by ^{28}Si and higher nuclei is ^{28}Si itself. Silicon, sulphur etc. partially melt-down into α -particles, neutrons and protons by photo-dissociation. These then participate in reaction networks involving quasi-equilibrium clusters linked by “bottleneck” links.

- Although beta decay and electron captures on stellar core nuclei do not produce energy in major ways they nevertheless play a crucial role in shifting the pathways of nuclear and thermodynamic evolution in the core conditions. These ultimately determine the mass of the core and its entropy structure which finally collapses in a supernova explosion.

8. Nucleosynthesis beyond Iron: neutron induced reactions

So far we have been dealing primarily with charged particle reactions and photodisintegration which lead to the production of lighter elements ($1 \leq A \leq 40$) and the recombination reactions for the production of elements $40 \leq A \leq 65$. However, the heavier elements ($A \geq 65$), because of their high charge and relatively weak stability, cannot be produced by these two processes. It was therefore natural to investigate the hypothesis of neutron

induced reactions on the elements that are formed already in the various thermonuclear burning stages, and in particular on the iron-group elements. The study of the nuclear reaction chains in stellar evolution shows that during certain phases large neutron fluxes are released in the core of a star. On the other hand, the analysis of the relative abundance of elements shows certain patterns which can be explained in terms of the neutron absorption cross-sections of these elements. If the heavier elements above the iron peak were to be synthesised during for example in charged particle thermonuclear reactions during silicon burning, their abundance would drop very much more steeply with increasing mass (larger and larger Coulomb barriers) than the observed behaviour of abundance curves which shows a much lesser than expected decrease. Based upon the abundance data of Suess and Urey ((56)), Burbidge et al ((14) hereafter B²FH) and independently Cameron ((15)) argued that heavy elements are made instead by thermal neutron capture.

These authors realised that two distinct neutron processes are required to make the heavier elements. The slow neutron capture process (s-process) has the lifetime for β -decay τ_β shorter than the competing neutron capture time τ_n (i.e. $\tau_\beta \leq \tau_n$). This makes the s-process nucleosynthesis run through the valley of β -stability. The rapid neutron capture r-process on the other hand requires $\tau_n \ll \tau_\beta$. This process takes place in extremely neutron-rich environments, for the neutron capture timescale is inversely proportional to the ambient neutron density. The r-process, in contrast to the s-process, goes through very neutron rich and unstable nuclei that are far off the valley of stability. The relevant properties of such nuclei are most often not known experimentally, and are usually estimated theoretically. Some of the key parameters are the half-lives of the β -unstable nuclei along the s-process path. But the nuclear half-life in stellar environment can change due to transitions from not just the ground state of the parent nucleus, but also because its excited states are thermally populated. In the r-process, the β -decay properties of the nuclei regulate the reaction flow to larger charge numbers and determine the resultant abundance pattern and the duration of the process. The r-process lasts for typically few seconds, in an intense neutron density environment: $n_n \sim 10^{20} - 10^{25} \text{cm}^{-3}$. In comparison, the neutron densities in the s-process are much more modest, say: $n_n \sim 10^8 \text{cm}^{-3}$; these neutron irradiation can take place for example in the helium burning phase of Red Giant stars. Nuclei above the iron group up to about $A = 90$ are produced in massive stars mainly by the s-process. Above $A = 100$ the s-process does very little in massive stars, although there are redistributions of some of the heavy nuclei. Most of the s-process above mass 90 is believed to come from Asymptotic Giant Branch stars. For a recent discussion of nucleosynthesis in massive stars, see Rauscher et al (46).

9. Conclusions

The nuclear reactions in the various stages of hydrostatic thermonuclear burning of massive stars have been discussed in this article. We discussed mainly the charged particle reactions, but also briefly mentioned the neutron induced reactions and photonuclear processes. What was discussed in the lectures, but could not be included in these notes was a description of the subsequent stage, i.e. the gravitational collapse of the core of the massive star under its own gravity that leads to a supernova explosion. These are extremely energetic explosions where the observable energy in the kinetic energy of the exploded debris and electromagnetic radiation add up to several times 10^{51} erg. The actual energy scale is typically 3×10^{53} erg or higher, but most of this is radiated away in neutrinos. Although the full understanding of the process of explosion in a gravitational collapse leading to a supernova has not been achieved despite several decades of theoretical and computational work, a watershed in the field was achieved observationally when a supernova exploded close by in a satellite galaxy of our own, namely SN1987A in the Large Magellanic Cloud (LMC). A few neutrinos were detected from this supernova, which were the first detections of the astrophysical neutrinos from outside of our solar system. By using the energetics of the neutrinos, their approximate spectral distribution, the distance to the LMC it was possible to show that the overall energy of the explosion was indeed $E_T \sim 2 - 3 \times 10^{53}$ erg. In addition, the duration of the neutrino burst was of the order of a few seconds as opposed to a few milliseconds, signifying that the observed neutrinos had to diffuse out of the dense and opaque stellar matter as predicted theoretically, instead of directly streaming out of the core. The spectral characteristics also indicated that the object that is radiating the neutrinos was indeed very compact, roughly of the same dimensions as that of a protoneutron star. Thus SN1987A provided the observational confirmation of the broad aspects of the theoretical investigation of stellar collapse and explosion. For a review of the understanding of the astrophysics of SN1987A, see (2).

Physicists are now gearing up to detect not only another supernova in our own galaxy, but by hoping to build very large neutrino detectors, they aim to detect supernova neutrinos from the local group of galaxies ((18), (19), (41)). As neutrinos from the supernova travel directly out from the core, they arrive a few hours ahead of the light flash from the exploding star, since electromagnetic radiation can only be radiated from the surface of the star, and it takes the supernova shock launched at the deep core several hours to travel to the surface. In the case of SN1987A, this time delay was useful in estimating the size of the star that exploded and was consistent with other (optical) spectroscopic data in this regard. Thus some advance warning ahead of the optical brightening of a supernova can be gotten from a “neutrino watch”. In AD 1604 when excitement arose over the discovery of what is to be later known as “Kepler’s supernova”, Galileo was criticised by the Padua city council, for

not having discovered it. Galileo apparently replied that he had more important things to do than to gaze out of the window, on the slim chance that he might catch something unusual (subsequently however, he participated in the lively discussions that took place about this new object in the sky). Physicists however would now be able to give an advance warning of an impending galactic supernova by a worldwide array of neutrino detectors connected loosely through the internet (SN Early Warning System or SNEWS¹⁰) which will notify astronomers to turn their optical, UV and other telescopes to the right direction when they find a burst of neutrinos characteristic of a supernova explosion. This advance warning will be of importance to catch the characteristics of the early ultraviolet and soft x-ray emission from the exploding star, in turn giving the structure of the outer layers of the progenitor star. Crucial input to the field of nuclear astrophysics is also coming from laboratory experiments involving radioactive ion beams (RIB). Short lived nuclei can only be studied close to their sites of formation before they decay away. Such complex facilities will further define through experimental input, the future of nuclear astrophysics.

Acknowledgments

I thank the organisers of the SERC School on Nuclear Physics, in particular, Prof. I. M. Govil for the invitation to visit Panjab University, Chandigarh where these lectures were given. I also thank him and Dr. R. K. Puri for their patience for this manuscript and Dr. B. K. Jain for his interest in the interface of nuclear physics and astrophysics. Dr. V. Nanal and P. Chandra are thanked for reading and commenting on the lecture notes. Research in nuclear astrophysics at Tata Institute is a part of the Plan Project: 10P-201.

REFERENCES

1. W. D. Arnett, *Supernovae and Nucleosynthesis*, Princeton University Press (1996).
2. W. D. Arnett, J. N. Bahcall, R. P. Kirshner, S. E. Woosley *Ann. Rev. Astron. Astrophys.*, **27** (1989), 629.
3. R. d'E. Atkinson, and F. G. Houtermans *Z. Phys.* **54** (1929) 656.
4. J. N. Bahcall, M. C. Gonzalez-Garcia, C. Pefia-Garay *Phys. Rev. Lett.* **90**, (2003) 131301.
5. J. N. Bahcall, L. S. Brow, A. Gruzinov and R. F. Sawyer *A. & S.* **383**, (2002) 291.

¹⁰See the site: <http://hep.bu.edu/~snnet/>

6. J. N. Bahcall, *Neutrino Astrophysics*, Chapter 3, Cambridge University Press (1989); see also Bahcall's web pages at: <http://www.sns.ias.edu/~jnb/>.
7. J. N. Bahcall and R. M. May *Ap. J.* **155**, (1969) 501.
8. J. N. Bahcall and C. P. Moeller *Ap. J.* **155**, (1969) 511.
9. H. A. Bethe and R.F. Bacher *Rev. Mod. Phys.* **8**, (1936) 82.
10. H. A. Bethe *Rev. Mod. Phys.* **9**, (1937) 69.
11. H. A. Bethe, and C. L. Critchfield *Phys. Rev.* **54** (1938) 248.
12. H. A. Bethe, and C. L. Critchfield *Phys. Rev.* **54** (1938) 862.
13. H. A. Bethe *Phys. Rev.* **55**, (1939) 103 and 434.
14. E. M. Burbidge, G. R. Burbidge, W. A. Fowler and F. Hoyle *Rev. Mod. Phys.* **29**, (1957) 547.
15. A. G. W. Cameron *Stellar Evolution, Nuclear Astrophysics and Nucleogenesis* (1957) Chalk River Report CRL-41.
16. B. J. Carr *Ann Rev Astr. Astrophys.* **419** (1994) 904.
17. B. J. Carr, J. Bond, and W. D. Arnett, *Ap. J.* **277** (1984) 445.
18. D. Casper *UNO A Next Generation Detector for Nucleon Decay and Neutrino Physics* meco.ps.uci.edu/lepton_workshop/talks/casper/uno.pdf (2000).
19. K. J. Chang *hep-ex/0005046* (2000).
20. N. Christlieb et al. *Nature* **419** (2002) 904.
21. D. D. Clayton, *Principles of Stellar Evolution and Nucleosynthesis*, University of Chicago Press (1984).
22. C. W. Cook, W. A. Fowler, C. C. Lauritsen, and T. Lauritsen, *Phys. Rev.* **107** (1957) 508.
23. R. Davis, D. S. Harmer, and K. C. Hoffman *Phys. Rev. Lett.* **20** (1968) 1205.
24. A. S. Eddington, *Observatory*, **43**, (1920), 341.
25. E. Fermi, *Nuclear Physics, Course Notes*, University of Chicago Press (1951), p.83.

26. B. W. Filippone, et al., *Phys Rev* **C28**, (1983), 2222.
27. W. A. Fowler *Proc. Welch Found. Conf. on Chemical Research*, ed. W.D. Milligan (Houston Univ. Press) (1977), p. 61.
28. E. Frieman and L. Motz, *Phys Rev* **89**, (1951), 648.
29. G. M. Fuller, W. A. Fowler and M. J. Newman, *Ap. J.*, **252** (1982), 715.
30. M. Guidry (1994) <http://csep10.phys.utk.edu/guidry/RIB-7-94html/cno.html>.
31. W. Haxton, *Nuclear Astrophysics Course* <http://ewiserver.npl.washington.edu/phys554/phys554.html> (1999).
32. C. Hayashi, R. Hoshi and D. Sugimoto, *Progr. Theor. Phys. Suppl.* **22**, (1951).
33. K. Hirata, T. Kajita, M. Koshiba, et al. *Physical Rev. Lett.*, **58**, (1987) 1490.
34. W. R. Hix and F. K. Thielemann *Ap. J.* **460**, (1996), 869.
35. F. Hoyle, *Ap. J. Sup.* **1**, (1954), 121.
36. F. Hoyle, D. N. F. Dunbar, W. A. Wenzel, and W. Whaling *Phys. Rev.* **92**, (1953), 1095.
37. K. Kar, S. Chakravarti, A. Ray and S. Sarkar *J. Phys. G.* **24**, (1998), 1641.
38. T. Kirsten, *The origin of the solar system*, ed. S. F. Dermott (New York: Wiley) (1978), p. 267.
39. K. Langanke and G. Martinez-Pinedo *nucl-th/0203071*, *Rev. Mod. Phys.* **75**, (2003), 819.
40. M. Mazarkis and W. Stephens, *Ap. J.* **171**, (1972) L97.
41. M. V. N. Murthy et al., *Pramana* **54**, (2002) 347.
42. J. A. Nolen and S. M. Austin, *Phys Rev*, C13, (1976), 1773.
43. E. J. Öpik, *Proc. Roy. Irish Acad.*, A54, (1951), 49.
44. Oak Ridge National Lab, *Nuclear Data for Nuclear Astrophysics* <http://www.phy.ornl.gov/astrophysics/data>
45. Lawrence Berkeley National Lab, *Nuclear Astrophysics Reaction Rates* <http://ie.lbl.gov/astro/astrorate.html>
46. T. Rauscher, A. Heger, R. D. Hoffman, and S. E. Woosley *Ap. J.*, 576, (1999) 323.

47. H. Reeves, *Stellar Evolution and Nucleosynthesis*, Gordon and Breach, New York (1968).
48. H. Reeves and E. E. Salpeter, *Phys. Rev.*, 116, (1959) 1505.
49. C. E. Rolfs and W. S. Rodney, *Cauldrons in the Cosmos*, University of Chicago Press (1988).
50. E. Rutherford, *Nature*, 123, (1929) 313.
51. G. K. Schenter and P. Vogel, *Nucl. Sci. Engg.*, 83, (1983) 393.
52. E. E. Salpeter, *Phys. Rev.*, 107, (1957) 516.
53. E. E. Salpeter, *Australian J. Phys*, 7, (1954) 373.
54. E. E. Salpeter, *Phys. Rev.*, 88, (1952) 547; also *Ap. J.*, 115, (1952), 326.
55. R. Salvaterra and A. Ferrara, *Mon. Not. Roy. Astr. Soc*, 340, (2003) L17.
56. H. E. Suess and H. C. Urey, *Rev. Mod. Phys.* 28, (1956) 53.
57. F. K. Thielemann and W. D. Arnett *Ap. J.*, 295, (1985) 264.
58. R. K. Wallace and S. E. Woosley, *Ap.J. Sup*, 45, (1981) 389.
59. L. van Wormer, J. Goerres, C. Iliadis, M. Wiescher & F. K. Thielemann, *Ap. J.* 432, (1994) 326.
60. C. F. von Weizsäcker, *Phys. Z.*, 38, (1937) 176.
61. C. F. von Weizsäcker, *Phys. Z.* 39, (1938) 633.
62. S. E. Woosley and T. A. Weaver, *Ann. Rev. Astr. Astrophys.*,24 (1986) 205.
63. A. E. Champagne and M. Wiescher, *Ann Rev. Nucl. Part. Sci* 42, (1992) 39.

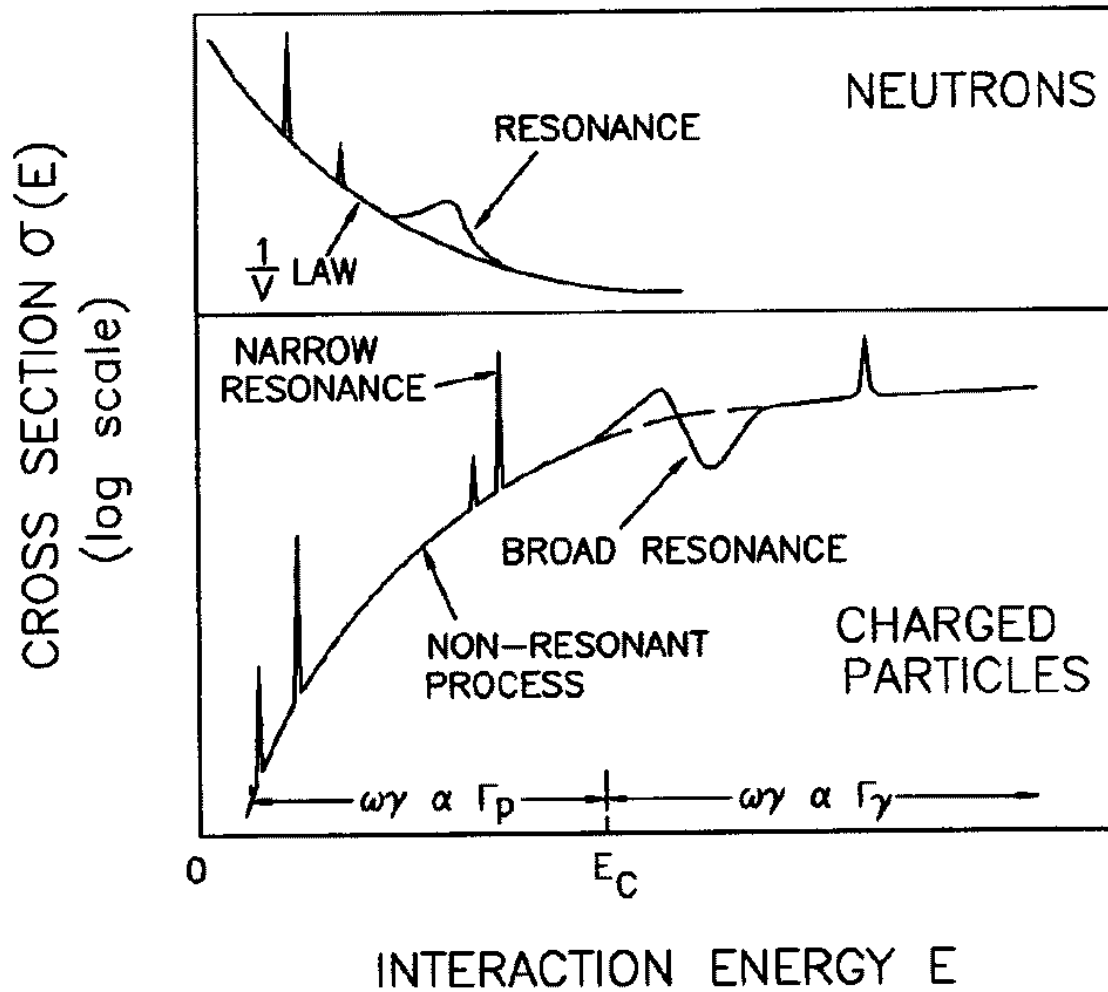


Fig. 1.— Dependence of total cross-sections on the interaction energy for neutrons (top panel) and charged particles (bottom panel). Note the presence of resonances (narrow or broad) superimposed on a slowly varying nonresonant cross-section (after (49)).

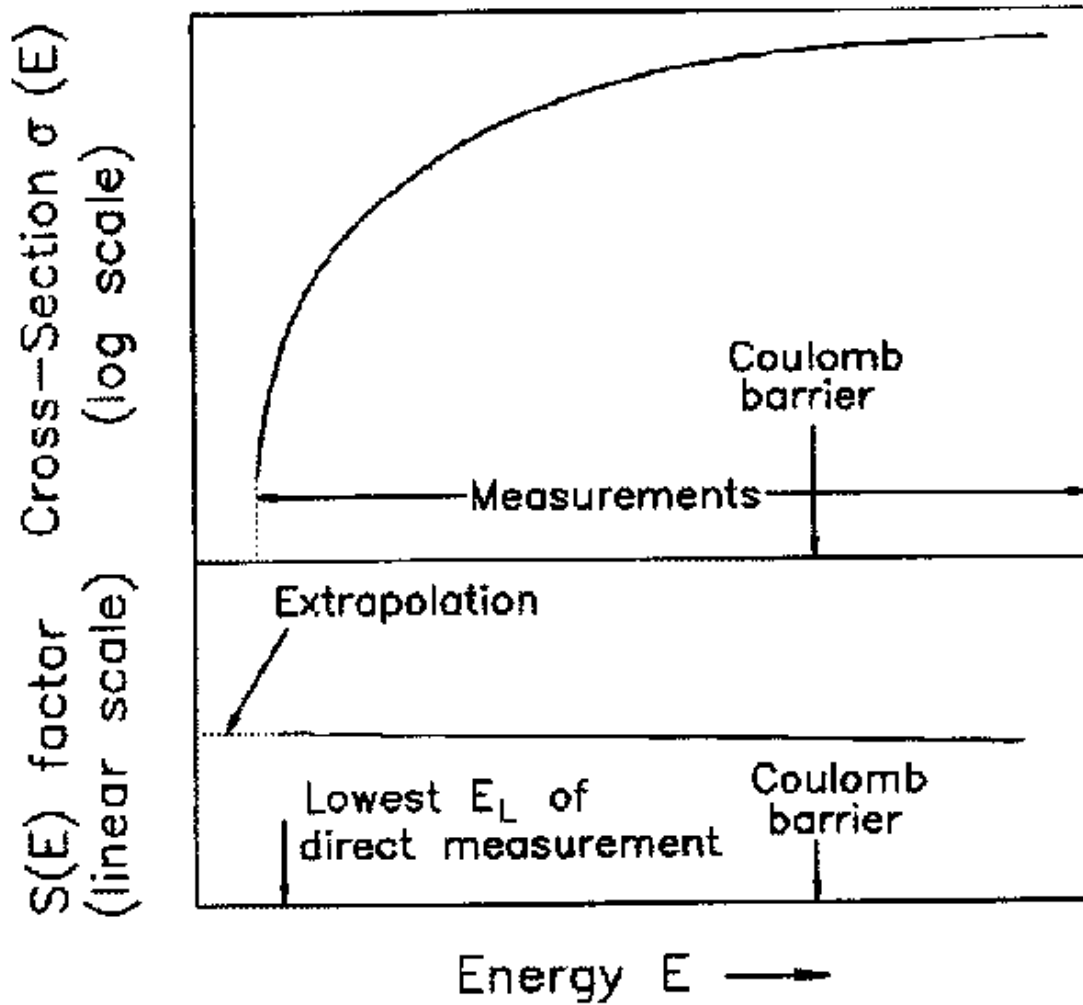


Fig. 2.— Cross-section and astrophysical S-factor for charged particle reactions as a function of beam energy. The effective range of energy in stellar interiors is usually far less than the Coulomb barrier energy E_C or the lower limit E_L where laboratory measurements can be carried out. Note that the scale is logarithmic for the cross-section but linear for S-factor, and hence the cross section drops sharply in the region of astrophysical interest, whereas the change is much less severe for the S-factor. Therefore, necessary extrapolation of laboratory data to lower energies relevant for astrophysical situations is more reliable in the case of S-factor.

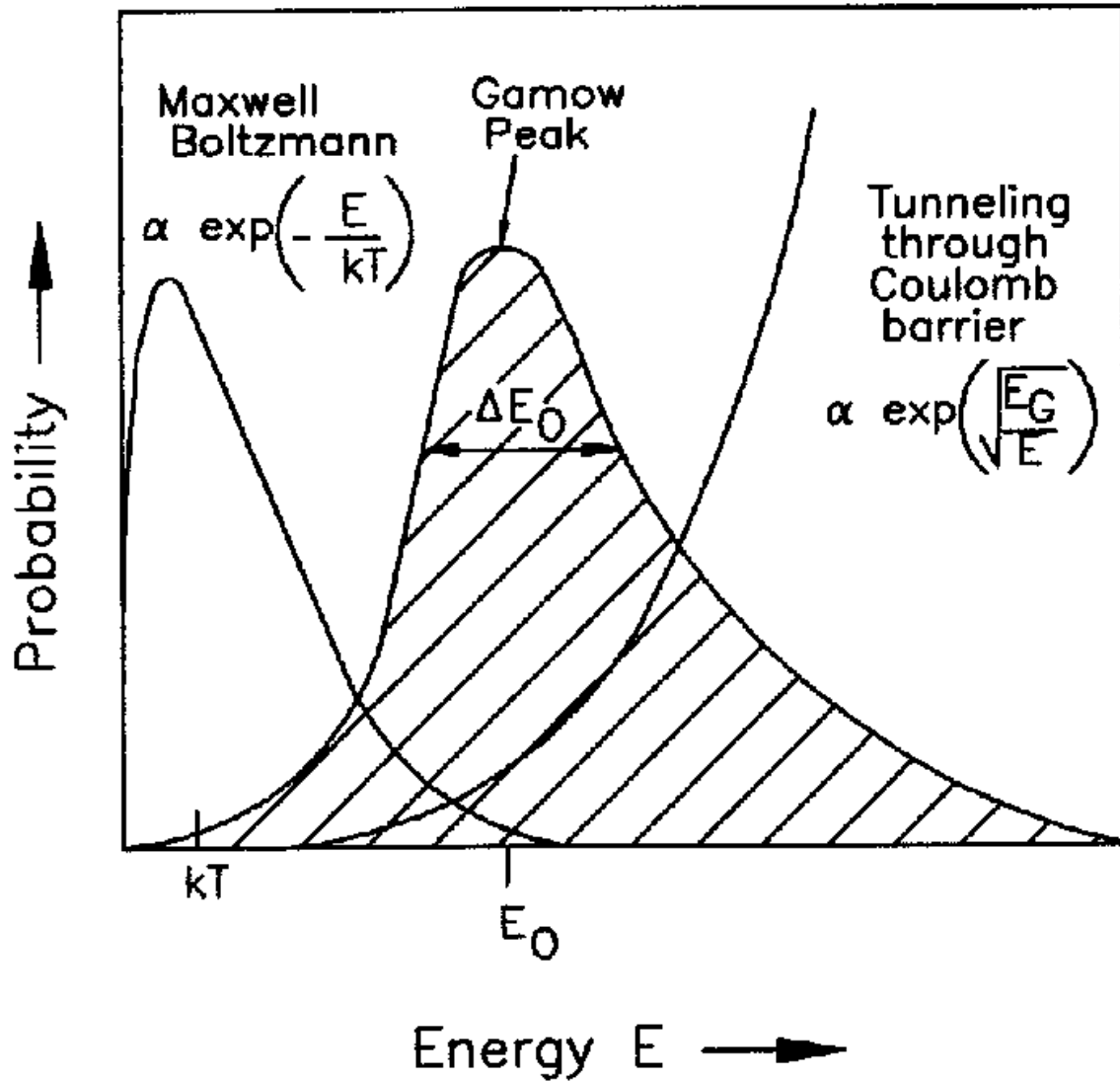


Fig. 3.— The Gamow peak is a convolution of the energy distribution of the Maxwell Boltzmann probability and the quantum mechanical Coulomb barrier transmission probability. The peak in the shaded region near energy E_0 is the Gamow peak that gives the highest probability for charged particle reactions to take place. Usually the Gamow peak is at a much higher energy than kT , and in the figure the ordinate scale (for the Gamow peak) is magnified with respect to those of the M-B and barrier penetration factors. See also Table 1.

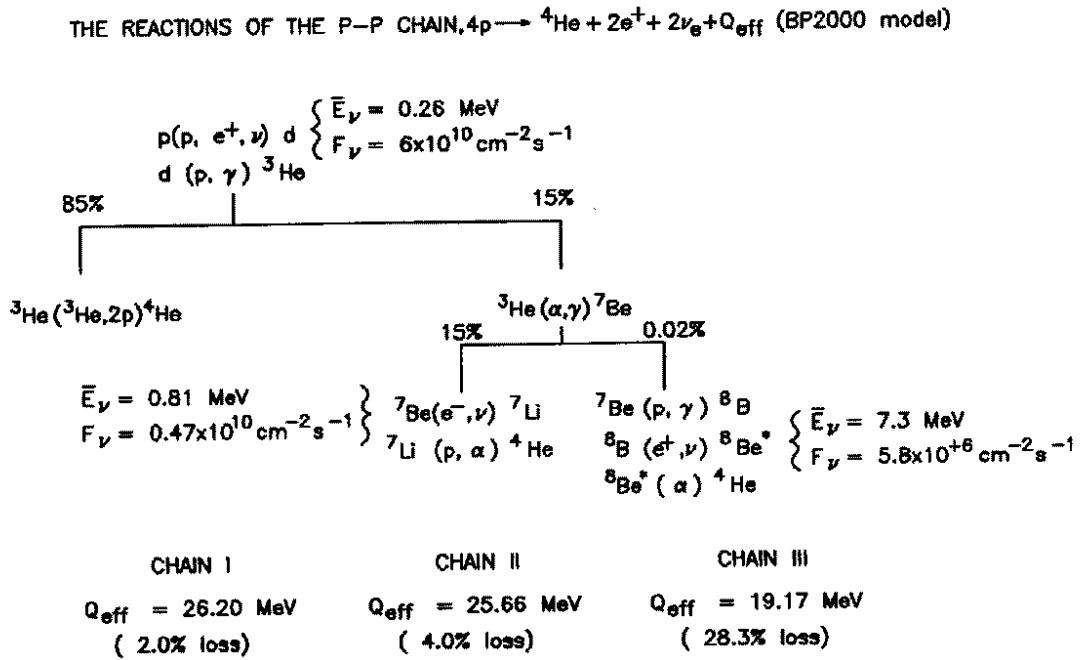


Fig. 4.— Reactions in the p-p chain start with the formation of deuterium and ${}^3\text{He}$. Thereafter, the ${}^3\text{He}$ is consumed in the sun 85% of the time through the ppI chain, whereas the ppII and ppIII chains together account for 15% of the time in the Bahcall Pinsonneault 2000 solar model. The ppIII chain occurs only 0.02% of the time, but the ${}^8\text{B}$ β^+ -decay provides the higher energy neutrinos (average $\bar{E}_\nu = 7.3 \text{ MeV}$). The net result of the chains is the conversion of four protons to a helium, with the effective Q-values (reduced from 26.73 MeV) as shown, due to loss of energy in escaping neutrinos.

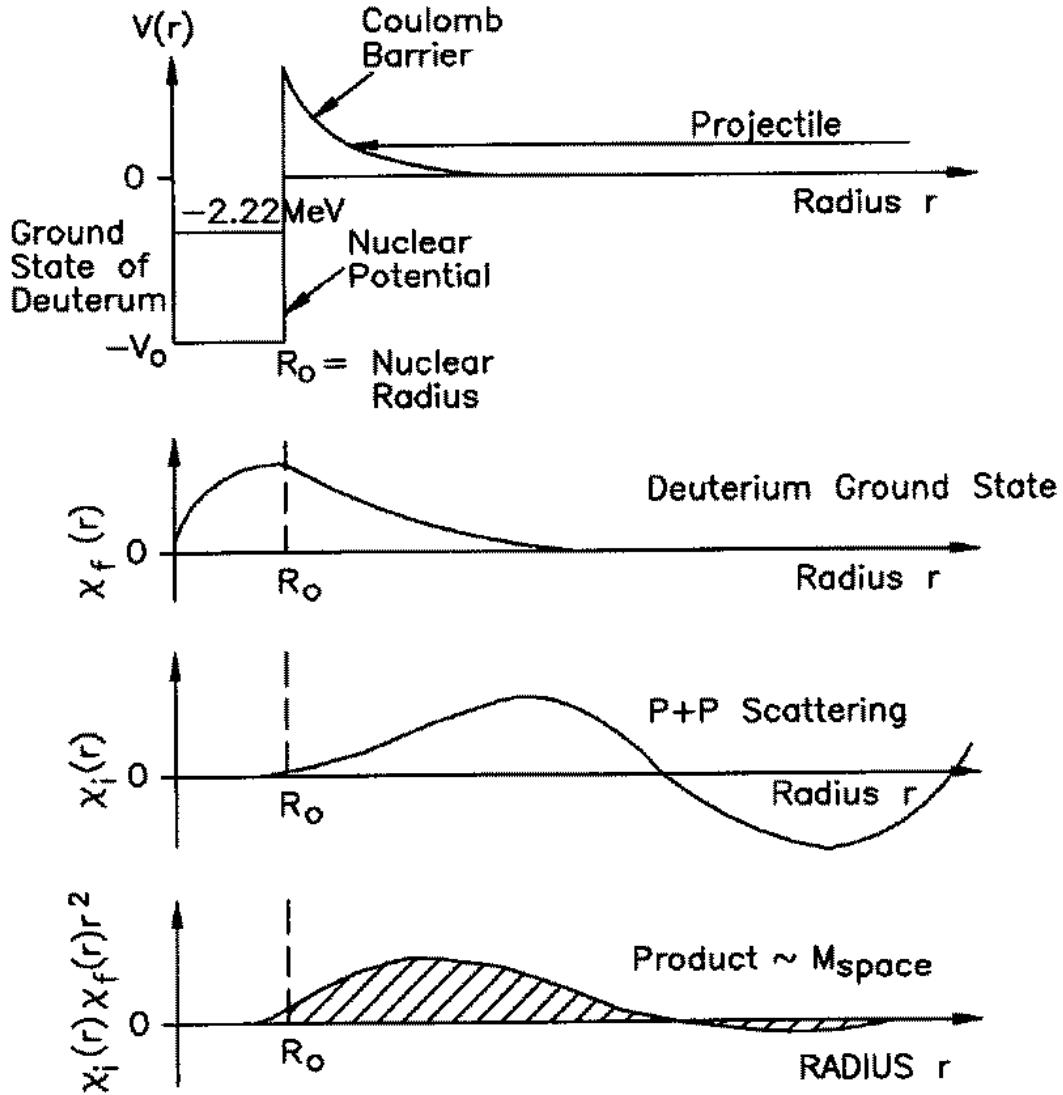


Fig. 5.— Schematic representation (after (49)) of the numerical calculation of the spatial part of the matrix element M_{space} in the $p + p \rightarrow d + e^+ + \nu_e$ reaction. The top part shows the potential well of depth V_0 and nuclear radius R_0 of deuterium with binding energy of -2.22 MeV . The next part shows the radius dependence of the deuterium radial wave function $\chi_d(r)$. The wavefunction extends far outside the nuclear radius with appreciable amplitude due to the loose binding of deuterium ground state. The p-p wavefunction $\chi_{pp}(r)$ which comprise the $l_i = 0$ initial state has small amplitude inside the final nuclear radius. The radial part of the integrand entering into the calculation of M_{space} is a convolution of both χ_d and χ_{pp} in the second and third panels and is given with the hatched shading in the bottom panel. It has the major contribution far outside the nuclear radius.

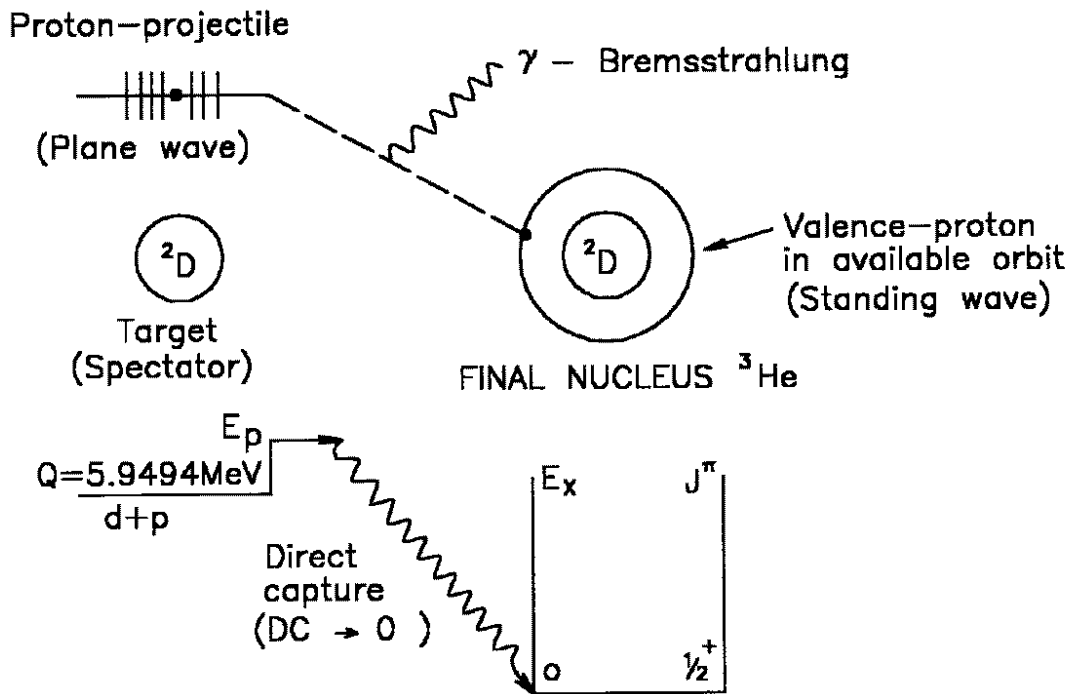


Fig. 6.— The Direct Capture reaction $d(p, \gamma)^3He$ to form 3He in its ground state. The proton projectile (shown as a plane wave) radiates away a bremsstrahlung photon to be captured in a “valence” orbital around the 2D .

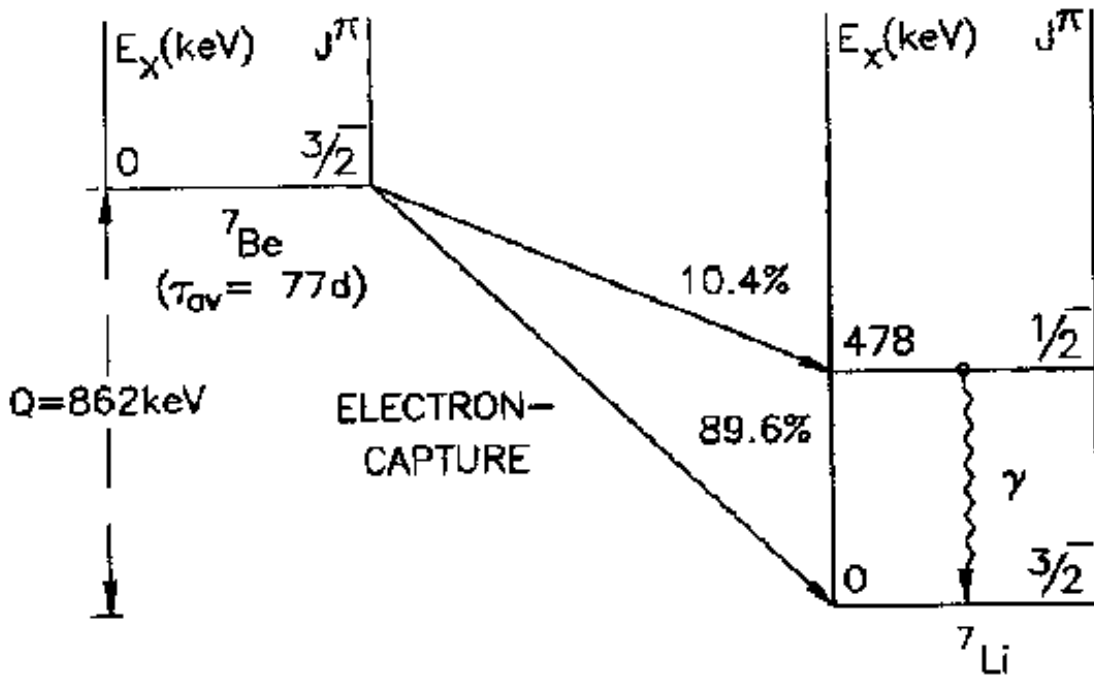


Fig. 7.— Electron capture on ${}^7\text{Be}$ nucleus. The capture proceeds 10.4% of the time to the first excited state of ${}^7\text{Li}$ at 478 keV, followed by a decay to the ground state by the emission of a photon. The average energy of the escaping neutrinos (which are from the ppII chain) is 814 keV.

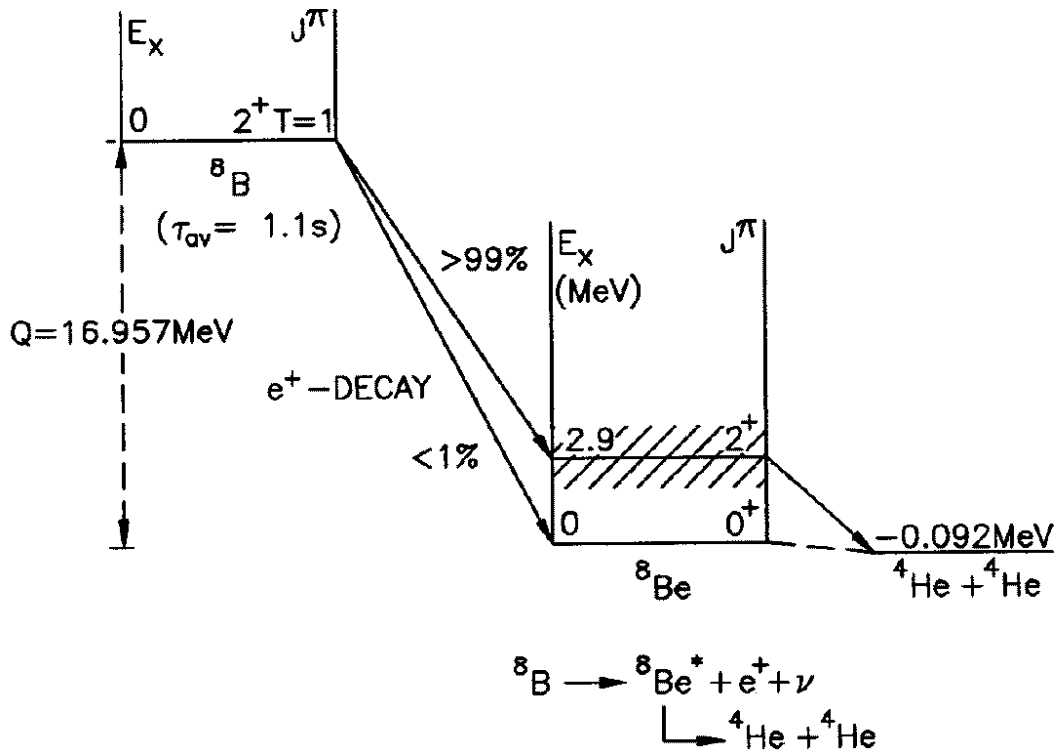


Fig. 8.— The decay scheme of ${}^8\text{B}$ with positron emission, which goes to the first excited state of ${}^8\text{Be}$ at $E_X = 2.9$ MeV with a width of $\Gamma = 1.6$ MeV. The ${}^8\text{Be}$ nucleus itself fissions into two alpha particles. The neutrinos accompanying the positron decay of ${}^8\text{B}$ are the higher energy solar neutrinos with $\bar{E}_\nu = 7.3$ MeV.

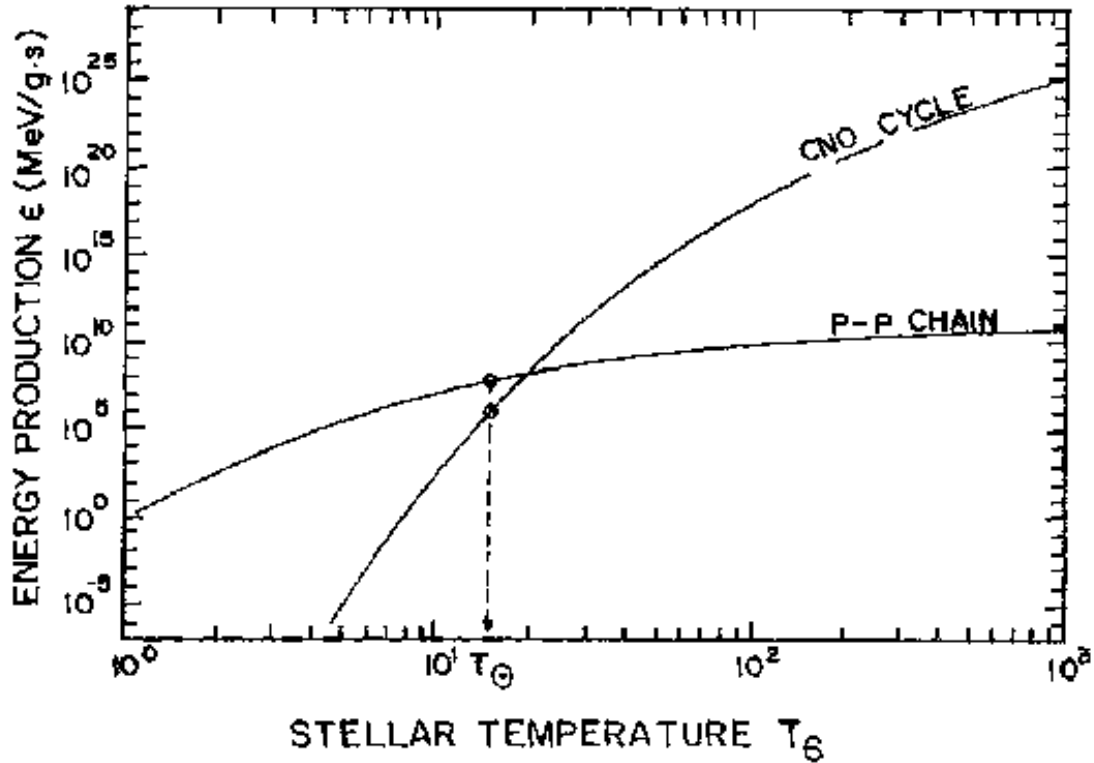


Fig. 9.— Comparison of the temperature dependence of the p-p chain and the CNO cycle energy production. The points marked for the solar central temperature $T_{\odot} = T_6 = 15$ are shown on both graphs. The CNO cycle generation dominates over the pp-chain at temperatures higher than $T_6 = 20$, so that for sun like stars, the pp-chain dominates. For more massive stars, the CNO cycle dominates as long as one of the catalysts: C, N, or O have initial mass concentration at least 1%. Note the logarithmic scales of the graph and how both rates drop sharply with decreasing temperature, with that of CNO cycle even more drastic due to higher Coulomb barriers.

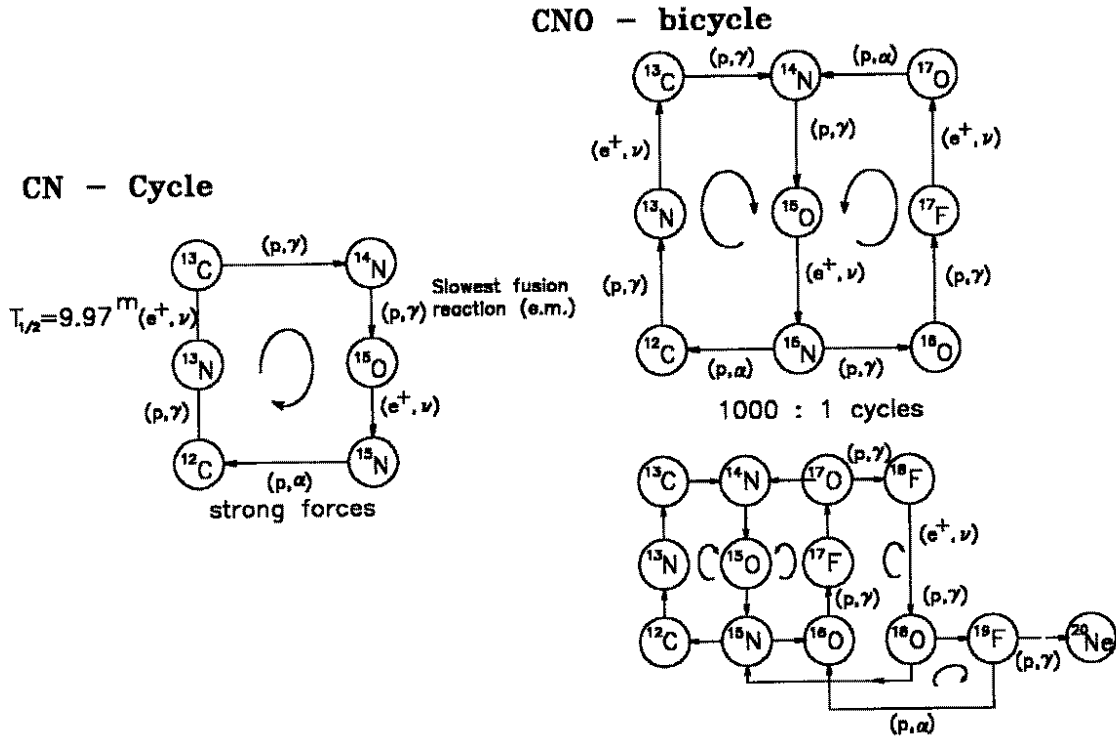


Fig. 10.— The various CNO cycles. The left part is the CN cycle where only C and N serve as catalysts for the conversion of four protons into ^4He . Here the slowest fusion reaction is (p,γ) reaction on ^{14}N whereas the slower β -decay has a half-life of 9.97m. In the CNO bicycle (right part), there is leakage from the CN cycle to the ON cycle through the branching at ^{15}N . The flow is returned to the CN cycle (which cycles 1000 times for each ON cycle) through $^{17}\text{O}(p,\alpha)^{14}\text{N}$. The right bottom part represents additional cycles linking into the CNO cycle through the $^{17}\text{O}(p,\gamma)^{18}\text{F}$ reaction (49).

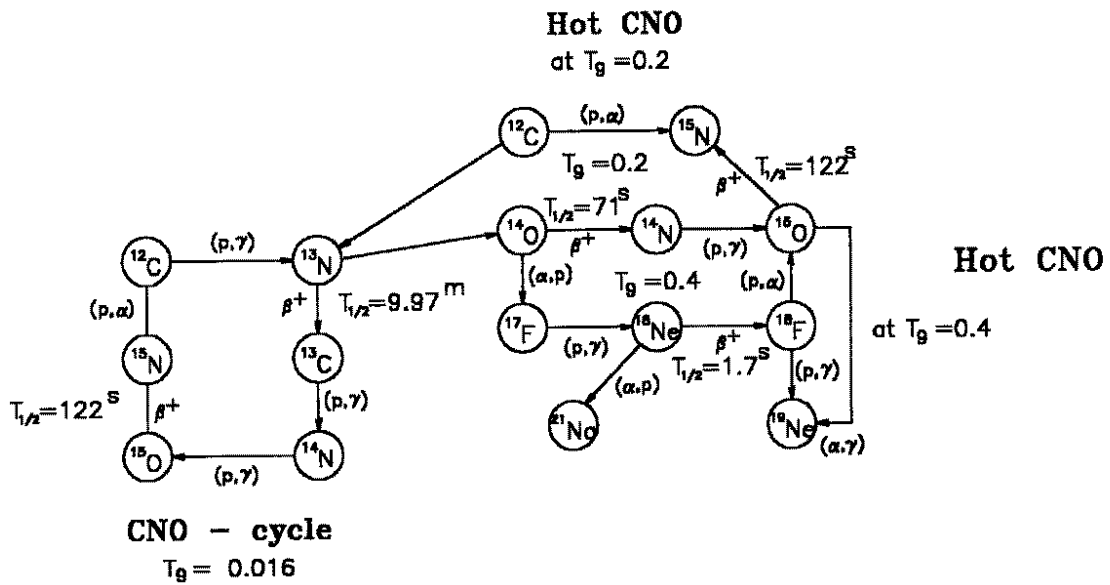


Fig. 11.— The “hot CNO” reaction schemes. While the “normal” CNO operates around $T_9 = 0.016$, at higher temperatures $T_9 \sim 0.2$, proton capture on ^{13}N can begin to compete with β -decay and the hot CNO ensues. At even higher temperatures $T_9 \sim 0.4$, reactions that break out of the CNO cycle compete. These breakouts are the beginnings of the rp-process.

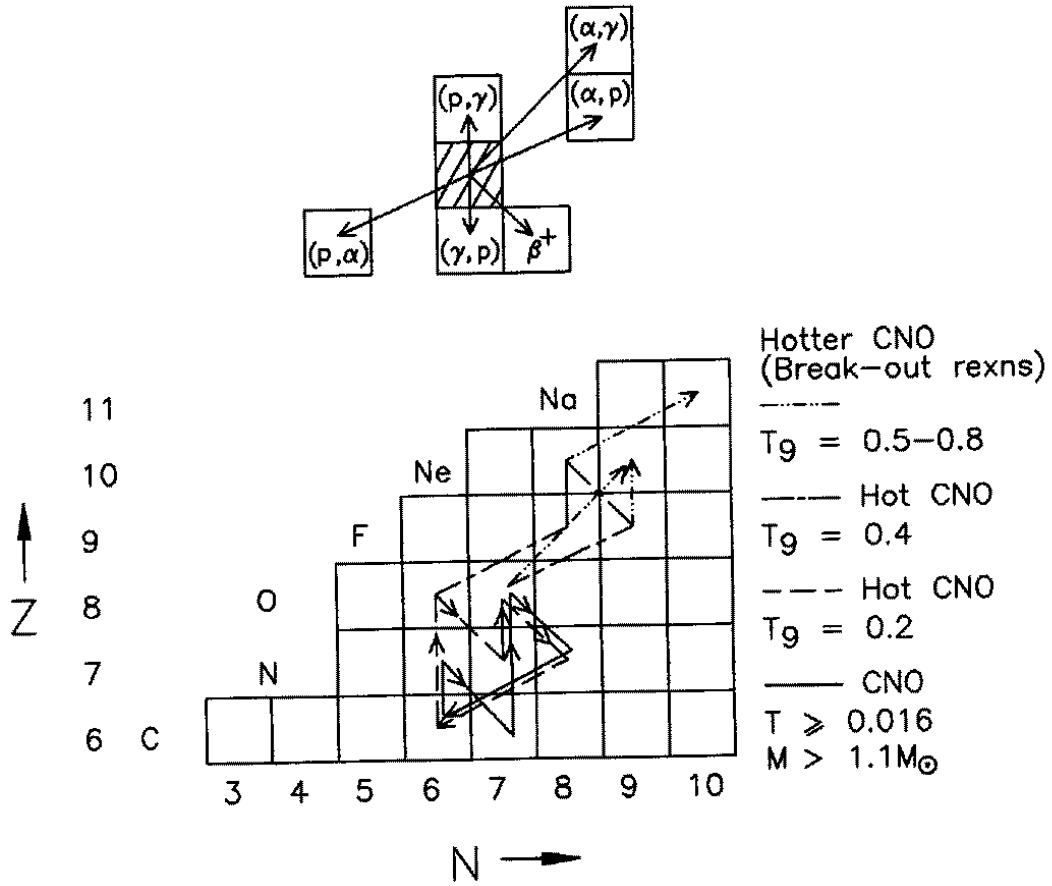


Fig. 12.— A given nucleus in the CNO cycles can participate in a variety of particle capture or emission reactions. The path in the (N, Z) plane for the CNO, hot CNO and breakout to rp-process are shown for successively higher temperatures.

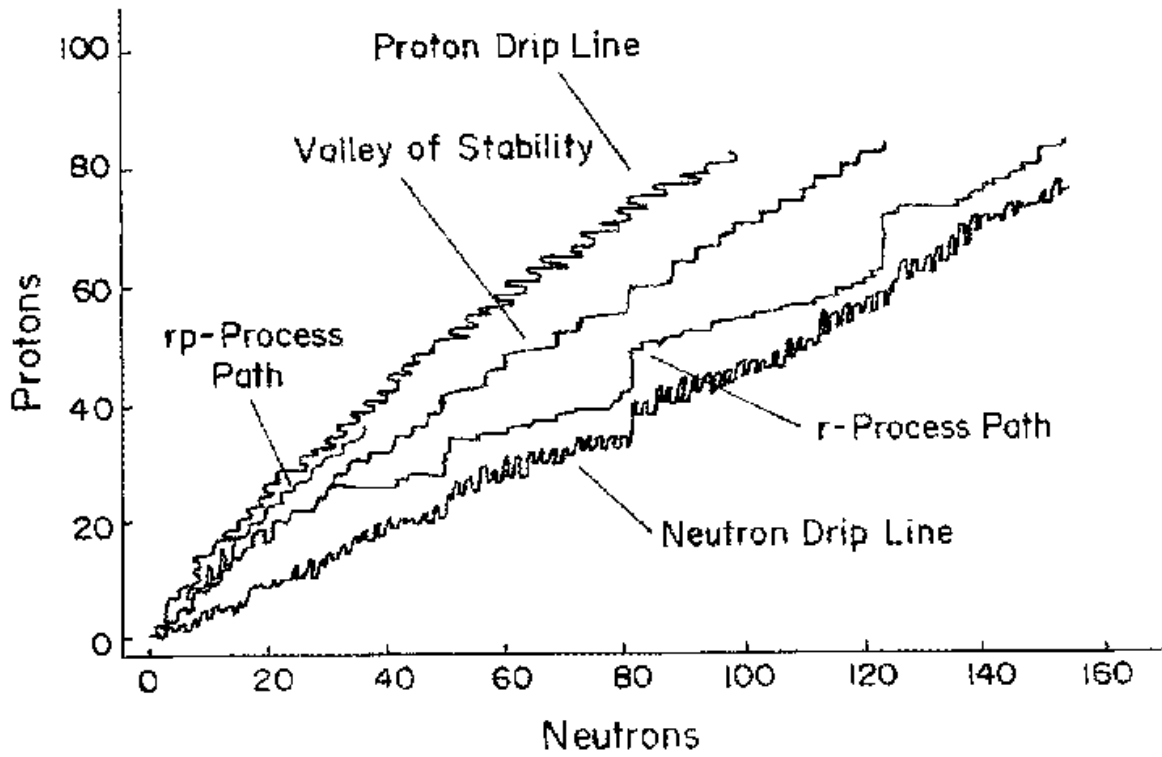


Fig. 13.— Schematic paths of r-process and rp-process in the (N,Z) plane with respect to the valley of beta-stability, the neutron drip and proton-drip lines.

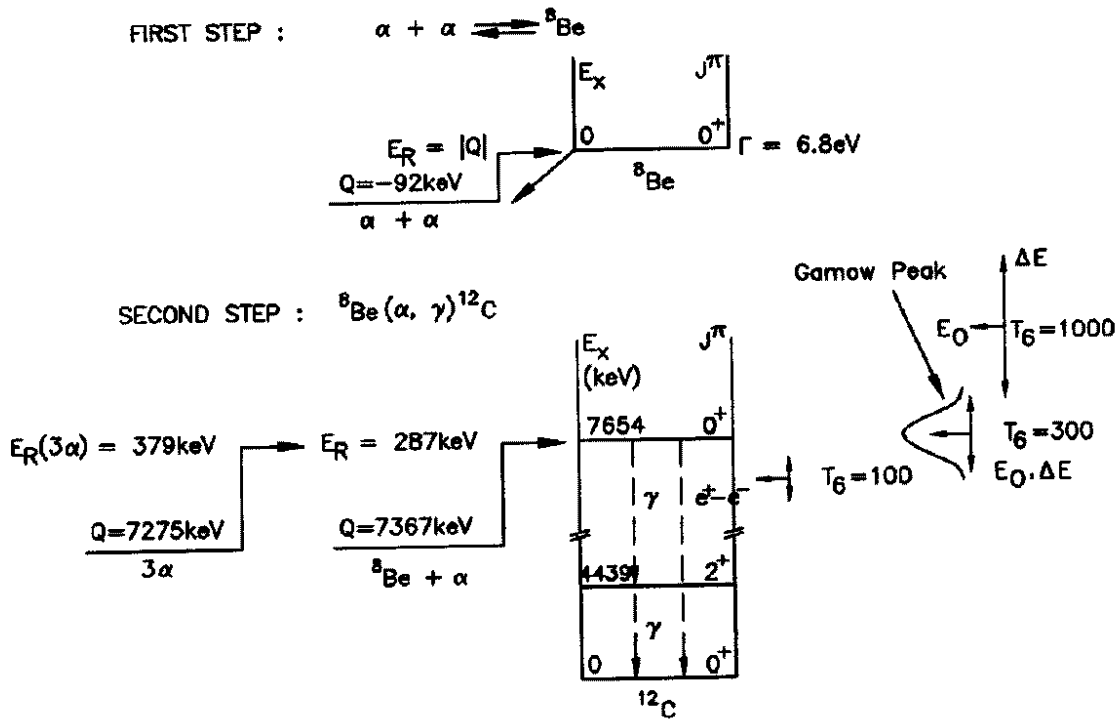


Fig. 14.— The triple alpha process of synthesising ${}^{12}\text{C}$ nucleus. In the first step a small amount of ${}^8\text{Be}$ nuclei build-up in equilibrium with its decay products (both forward and backward reactions involve alpha particles). The second step involves a capture of another alpha particle by the unstable ${}^8\text{Be}$ nucleus which proceeds via an s-wave resonance state in the product nucleus ${}^{12}\text{C}$ which is located close to the Gamow energy regions for temperatures indicated schematically by the three-way arrows on the right.

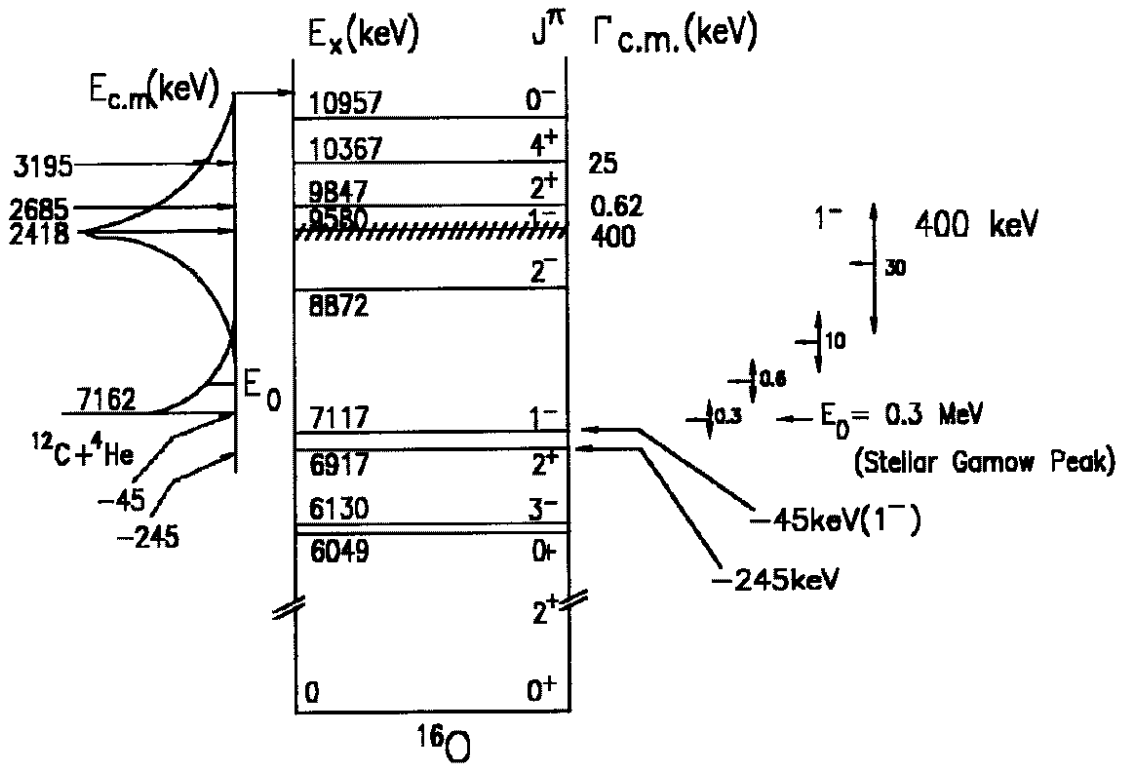


Fig. 15.— Energy levels of ^{16}O nucleus near and above the alpha-particle threshold of capture on ^{12}C . Shown on the right are effective stellar energy regions corresponding to the temperatures given near the three-way arrows. The reaction rate is influenced mainly by the high energy tails of two subthreshold resonances in ^{16}O at $E_R = -45$ keV and $E_R = -245$ keV, plus the low energy tail of another high-lying broad resonance at 9580 keV.

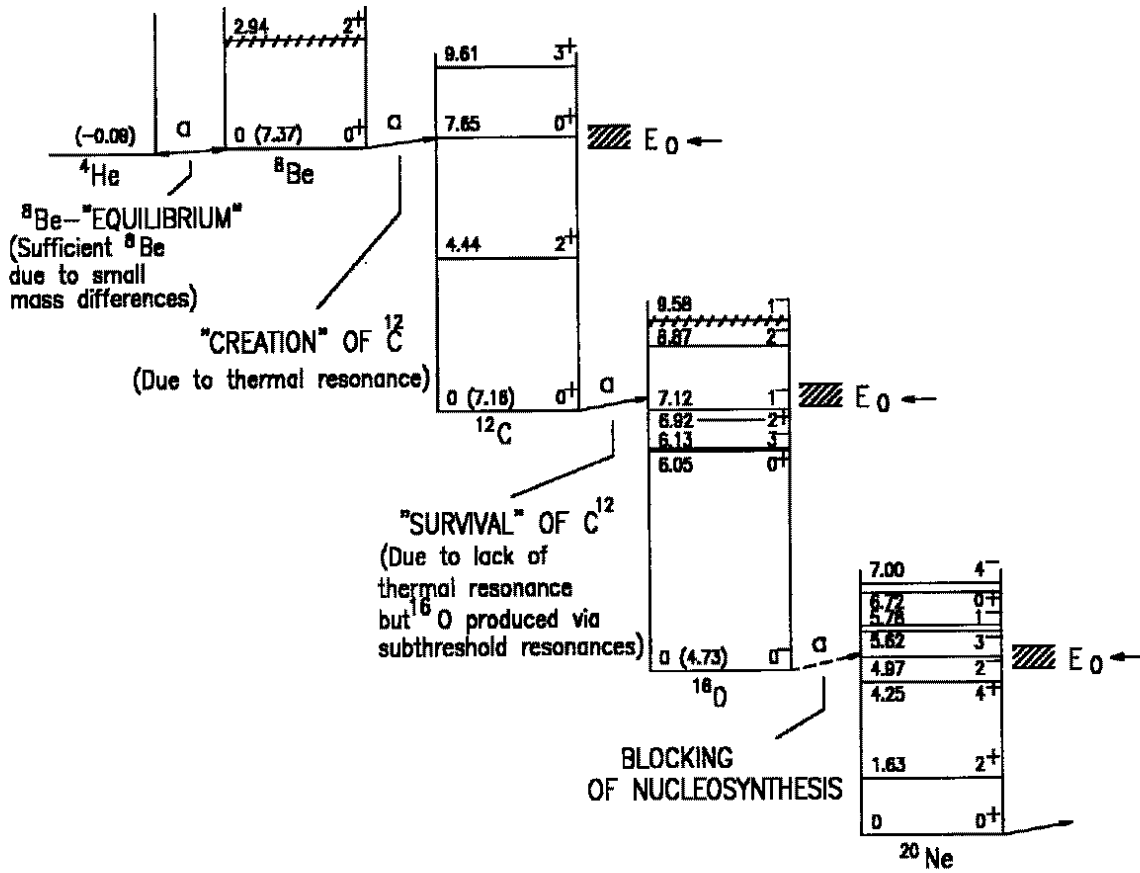


Fig. 16.— Energy levels of nuclei participating in thermonuclear reactions during the helium burning stage in red giant stars (after (49)). The survival of both ${}^{12}\text{C}$ and ${}^{16}\text{O}$ in red giants, believed to be the source of terrestrial abundances depends upon fortuitous circumstances of nuclear level structures and other properties in these nuclei.

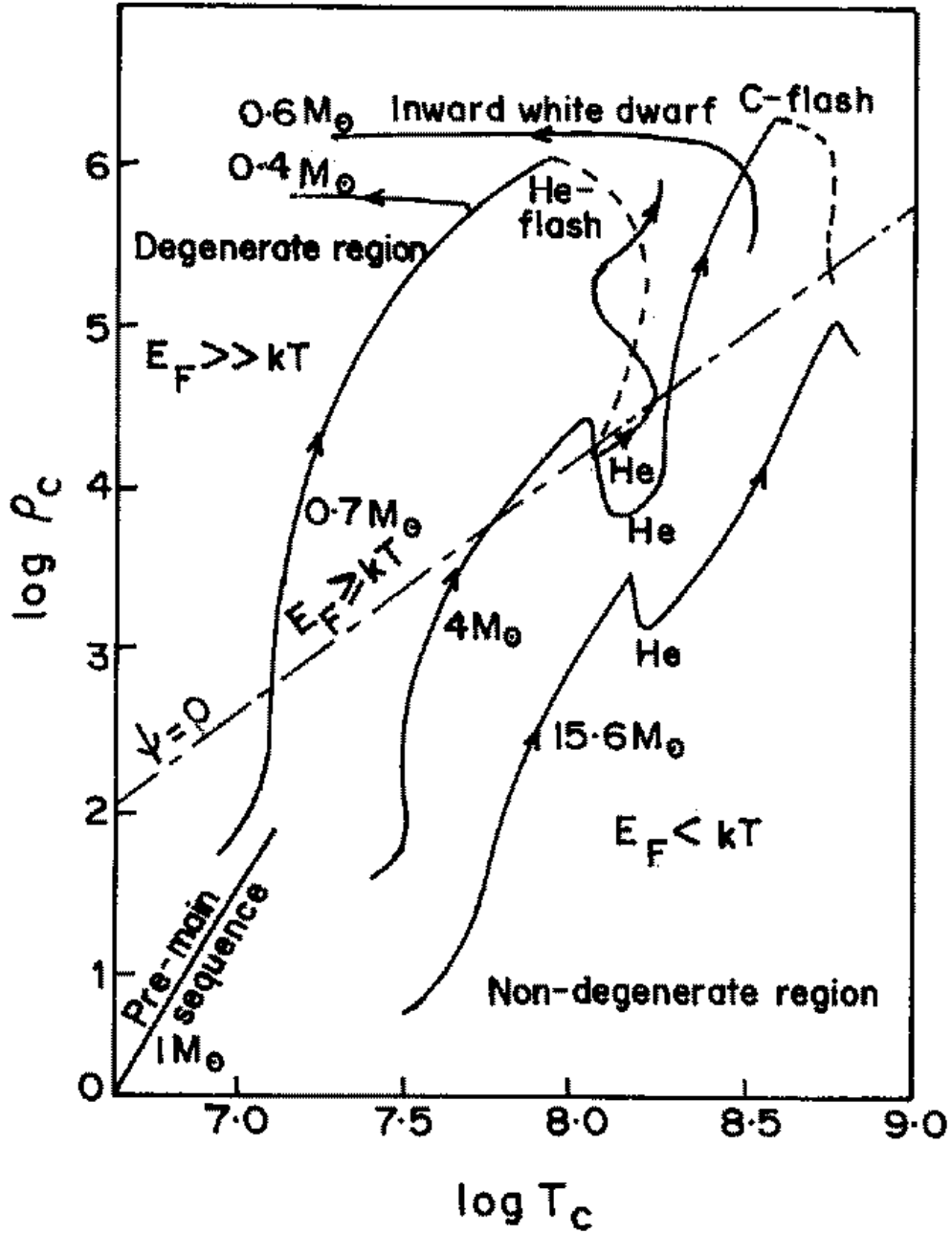


Fig. 17.— Tracks in the core temperature, density plane of stars of various masses (at the start of hydrogen burning i.e. main sequence masses). Note that a star of mass $M \sim 15M_\odot$ ignites all its fuels in non-degenerate conditions, whereas a star of mass $M \sim 4M_\odot$ ignites carbon under strongly degenerate conditions. (After (32)).